

Quasistatic propagation of steps along a phase boundary

Basant Lal Sharma ^{*} Anna Vainchtein [†]

Abstract

We study quasistatic propagation of steps along a phase boundary in a two-dimensional lattice model of martensitic phase transitions. For analytical simplicity, the formulation is restricted to antiplane shear deformation of a cubic lattice with bi-stable interactions along one component of shear strain and harmonic interactions along the other. Energy landscapes connecting equilibrium configurations with periodic and non-periodic arrangements of steps are constructed, and the energy barriers separating metastable states are calculated. We show that a sequential one-by-one step propagation along a phase boundary requires smaller energy barriers than simultaneous motion of several steps.

Keywords: phase boundary, steps, energy landscape, energy barrier

1 Introduction

Although they may appear planar on the macroscopic level, martensitic phase boundaries typically contain multiple steps, or ledges. A long-standing hypothesis in materials science states that a phase boundary moves forward via a propagation of steps *along* the interface [6, 7]. Recent experimental observations confirm this hypothesis: for example, Bray and Howe [1] found the fcc/hcp martensite transformation in Co-Ni occurs by the passage of Shockley partial dislocation ledges and that the hcp martensite thickens by the lateral movement of ledges across the fcc/hcp interface. The mechanism of step motion thus largely determines the kinetics of martensitic phase boundaries, which in turn determines the dissipative properties of active materials undergoing such transformations.

^{*}Department of Mechanical Engineering, Indian Institute of Technology Kanpur, Kanpur, U. P. 208016, India

[†]Department of Mathematics, University of Pittsburgh, Pittsburgh, PA 15260

Let us consider the following thought experiment. Suppose a material body contains a phase boundary with a large number of steps. Consider an external loading that is so slow that inertial effects can be neglected. In this case the propagation of steps, and hence the phase boundary, is quasistatic and can be represented by a series of equilibrium configurations connected by non-equilibrium paths that go through energy barriers separating the equilibria. In this situation we expect that a simultaneous motion of a large number of steps would involve a much higher energy barrier than a motion in which these steps move one at a time. In this paper we show that this hypothesis is in fact justified by directly calculating the energy barriers associated with both types of motion under certain simplifying assumptions.

Specifically, we consider a staircase-like phase boundary in a three-dimensional cubic lattice undergoing an antiplane shear deformation. This reduces the model to, effectively, a two-dimensional lattice deforming out of its plane. To model phase transitions in a simple way that allows explicit analytical calculations, we assume that a bi-parabolic potential governs the interaction in the vertical bonds, with the two parabolas representing two different material phases with same vertical shear moduli, while the horizontal bonds are harmonic. The shear moduli in horizontal and vertical directions may differ, modeling material anisotropy. Under these assumptions, we use techniques developed by Duffin [4] and Maradudin [12] to construct stable (in the sense of local energy minimum) equilibrium configurations with a phase boundary that has a rational slope and therefore consists of periodically distributed steps. We then construct a Green's function that allows us to obtain stable equilibria with a local break in periodicity that lie near the periodic states in the energy landscape. For each of these states, we can compute the range of applied strains under which these equilibria exist, similar to the propagation failure range studied by Cahn et al. [2] for a different two-dimensional lattice model. This range depends on the slope of the phase boundary and the material anisotropy.

Generalizing the approach used in Fedelich and Zanzotto [5] and Truskinovsky and Vainchtein [13] for a one-dimensional chain of bi-stable springs (see also the related work of Hobart [8, 9, 10, 11] for the Frenkel-Kontorova dislocation model), we construct non-equilibrium paths connecting the neighboring periodic and non-periodic energy minima in the present two-dimensional lattice model, with a finite number n of vertical bonds changing phase along a path. Among all possible paths connecting two neighboring equilibria, we select the one that involves a minimal (Peierls) energy barrier. The key ingredient in our construction is the vector order parameter describing the phase change along the path. The construction projects the infinite-dimensional energy landscape on an n -dimensional surface that includes neighboring equilibria with different locations of steps along the phase boundary. This allows us to compute the minimal energy barriers separating the equilibria and compare the energy barriers along different paths.

We apply our construction to a specific example involving the quasistatic motion of n

neighboring steps along a phase boundary with integer slope and consider two different paths connecting the initial and final states at a fixed applied strain. Along the first path, the steps are allowed to move simultaneously, while the second path involves one-by-one, or sequential, step propagation. We show that the energy barrier for the propagation of an initial one step along the second path is smaller than the energy barrier needed to initiate the simultaneous step propagation along the first path; in fact, our calculations show that the ratio of two energy barriers is close to n . In addition, we show that depending on the material anisotropy parameter χ and the slope μ of the phase boundary, the energy barriers along the sequential path can either increase, decrease or reach a maximum value. In particular, sufficiently small χ results in energy barriers decreasing along the path, so that overcoming the energy barrier to move an initial one step indeed results into a cascade motion of the subsequent steps sequentially. For higher material anisotropy parameter χ , the largest energy barrier occurs further along the path. This may result in arresting the motion if the system does not have enough energy to overcome all energy barriers; however, the largest energy barrier decreases as χ grows.

Our analysis suggests that there are purely energetic reasons for the steps to propagate sequentially along a phase boundary under quasistatic loading. Recent analysis and simulations of the full dynamic problem [14, 15] show that sequential motion is also preferred when step velocities are sufficiently high.

The paper is organized as follows. In Section 2 we formulate the lattice model. Periodic solutions with integer slope are found in Section 3, and the results are generalized to the case of rational slope in Section 4. Neighboring non-periodic solutions are obtained in Section 5. In Section 6 we construct a minimal barrier path connecting a periodic equilibrium to the lower energy non-periodic state obtained by moving one step. The procedure is generalized to the case of finite number of steps and a vector order parameter in Section 7. Our main results for sequential and simultaneous step propagation for the case of integer slope are presented in Section 8, and in Section 9 we consider an example illustrating these results. Section 10 is devoted to concluding remarks. Proofs and technical results can be found in appendices.

2 Lattice Model

Consider an antiplane shear deformation of a cubic lattice with interatomic distance ε . This means that the problem can be equivalently formulated as an out-of-plane deformation of a two-dimensional lattice of rigid columns. The columns will be henceforth referred to as “particles”. Let \mathbb{Z} denote the set of integers. Let $w_{m,n}$ denote the out-of-plane displacement of the (m,n) th particle where $m, n \in \mathbb{Z}$. We take into account only nearest-neighbor interactions between the particles and assume that these are modeled

by elastic springs with energy densities (per unit length) $\phi_h(u)$ for horizontal springs and $\phi_v(v)$ for vertical ones. Here u and v are the horizontal and vertical components of the antiplane shear strain. Note that the two energy densities are in general different due to anisotropy of the crystal lattice. The elastic energy of the system is then given by

$$E(\{w_{m,n}\}_{m,n \in \mathbb{Z}}) = \varepsilon \sum_{m,n} \phi_h\left(\frac{w_{m,n} - w_{m,n-1}}{\varepsilon}\right) + \phi_v\left(\frac{w_{m,n} - w_{m-1,n}}{\varepsilon}\right), \quad (1)$$

and the equilibrium equations are

$$\begin{aligned} & \phi_h'\left(\frac{w_{m+1,n} - w_{m,n}}{\varepsilon}\right) - \phi_h'\left(\frac{w_{m,n} - w_{m-1,n}}{\varepsilon}\right) \\ & + \phi_v'\left(\frac{w_{m,n+1} - w_{m,n}}{\varepsilon}\right) - \phi_v'\left(\frac{w_{m,n} - w_{m,n-1}}{\varepsilon}\right) = 0. \end{aligned} \quad (2)$$

To model phase transitions, we now assume that the vertical springs are bi-stable, i.e. they can exist in two different phases (phase variants), each corresponding to a potential well of $\phi_v(v)$. To simplify analysis, we further assume the two-parabola potential

$$\phi_v(v) = \frac{1}{2}K_v v^2 - K_v a(v - v_c)\theta(v - v_c), \quad (3)$$

where $K_v > 0$ is the elastic modulus in each well, $a > 0$ is the transformation strain and $\theta(v)$ is a unit step function. The critical strain v_c separates phase I ($v < v_c$) from phase II ($v > v_c$) for the vertical springs. Meanwhile, the horizontal springs are assumed to be linearly elastic, with

$$\phi_h(u) = \frac{1}{2}K_h u^2, \quad (4)$$

where $K_h > 0$ is the elastic modulus for these springs.

To reduce the number of parameters, it is convenient to rescale the problem, introducing dimensionless variables $\bar{w}_{m,n} = w_{m,n}/(a\varepsilon)$, $\bar{\phi} = \phi/K_v$ and parameters $\chi = K_h/K_v > 0$, dimensionless measure of material anisotropy, and $\bar{v}_c = v_c/a$, dimensionless critical strain. After dropping the bars we obtain

$$\phi_h(u) = \frac{1}{2}\chi u^2, \quad \phi_v(v) = \frac{1}{2}v^2 - (v - v_c)\theta(v - v_c), \quad (5)$$

and the equilibrium equations (2) become

$$\begin{aligned} & \chi(w_{m+1,n} + w_{m-1,n} - 2w_{m,n}) + (w_{m,n+1} + w_{m,n-1} - 2w_{m,n}) \\ & = \theta(w_{m,n+1} - w_{m,n} - v_c) - \theta(w_{m,n} - w_{m,n-1} - v_c) \end{aligned} \quad (6)$$

In addition we assume that at infinity the solution satisfies certain far-field boundary conditions, to be specified later, that correspond to homogeneous deformation in each phase.

In this paper we consider equilibrium configurations with a single phase boundary that contains *steps* and focus our attention on how these steps evolve as we change the boundary conditions.

3 Phase boundary with a periodic array of steps: integer slope

We begin by considering equilibrium configurations with a single phase boundary that consists of a periodic array of steps of length $\mu \geq 1$ and unit height each, as shown in the Fig. 1. The vertical springs below and along the steps are in phase II, while the springs

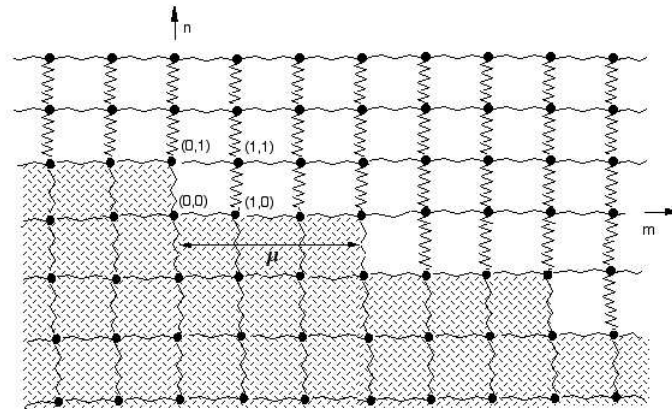


Figure 1: A phase boundary with periodic steps. Here the period μ is an integer.

above are in phase I. In this simplest case the slope of the phase boundary is the integer μ . Later we will consider more general periodic configurations in which the slope is a rational number.

It is convenient to introduce vertical strains $v_{m,n}$ that measure the deformation of the bi-stable vertical springs and are related to the out-of-plane displacements $w_{m,n}$ via

$$v_{m,n} = w_{m,n} - w_{m,n-1}.$$

Subtracting from (6) the equation obtained by replacing n in (6) by $n - 1$, we obtain the equilibrium equations in terms of vertical strains only:

$$\begin{aligned} & \chi(v_{m+1,n} + v_{m-1,n} - 2v_{m,n}) + (v_{m,n+1} + v_{m,n-1} - 2v_{m,n}) \\ & = \theta(v_{m,n+1} - v_c) - 2\theta(v_{m,n} - v_c) + \theta(v_{m,n-1} - v_c). \end{aligned} \quad (7)$$

We will solve (7) subject to the condition that vertical strains tend to constant values at infinity:

$$v_{m,n} \rightarrow v_{\pm} \quad \text{as } m \rightarrow \pm\infty \text{ for a fixed } n. \quad (8)$$

As we shall see shortly, due to the force equilibrium the strains v_{\pm} are not independent, so that only one of these can be prescribed (say, v_-) by controlling the vertical component of stress at infinity.

We assume an equilibrium with a single phase boundary. If the phase boundary is horizontal ($\mu = \infty$), the problem (7), (8) is trivially solved by the piecewise constant vertical strain

$$v_{m,n} = \begin{cases} v_+, & n > n_0 \\ v_-, & n \leq n_0, \end{cases} \quad (9)$$

where $n = n_0$ is the location of the phase boundary and we have $v_+ = v_- - 1$, $v_+ < v_c$, $v_- > v_c$. Thus in what follows we will assume a non-flat phase boundary with $1 \leq \mu < \infty$. As we shall see, the periodic step arrangement creates a boundary layer around the phase boundary and oscillations that die away from it, in agreement with (8).

Note that due to our special choice (5) of interaction potentials, the left hand side of the system (7) is linear, with nonlinearity in the right hand side given by a combination of unit step functions that depend on the unknown strains. However, for a given phase boundary location the nonlinear right hand side can be written as a combination of Kronecker delta functions $\delta_{m,n}$ (equal to 1 if $m = n$ and zero otherwise). In particular, for the periodic ansatz such as shown in Fig. 1, (7) reduces to

$$\begin{aligned} & \chi(v_{m+1,n} + v_{m-1,n} - 2v_{m,n}) + (v_{m,n+1} + v_{m,n-1} - 2v_{m,n}) \\ & = - \sum_p \sum_{l=1}^{\mu} \delta_{m,l-p\mu} (\delta_{n,p} - \delta_{n-1,p}), \end{aligned} \quad (10)$$

where the index p in the left hand side fixes the step and the index l fixes the particle in each step of the phase boundary.

Taking discrete Fourier transform of both sides of the equation (10), we obtain

$$\hat{v}(x, y) = \frac{\pi \sum_q \delta(y - \mu x - 2\pi q)(1 - e^{iy})(e^{i\mu x} - 1)}{2(1 - e^{-ix})(\chi \sin^2 \frac{x}{2} + \sin^2 \frac{y}{2})}, \quad (11)$$

where $\delta(\cdot)$ is the Dirac delta (generalized) function, x, y are the wave numbers, and $\hat{v}(x, y)$ is the (generalized) Fourier transform of $v - v_-$ formally defined by

$$\hat{v}(x, y) = \sum_{m,n} (v - v_-) e^{ixm + iyn}. \quad (12)$$

To obtain (11) we used the identity

$$\sum_p e^{ipz} = 2\pi \sum_q \delta(z - 2\pi q), \quad (13)$$

which holds for any real z . Due to the sum of Dirac delta functions in the right hand side of (11), the inverse Fourier transform

$$v_{m,n} = v_- + \frac{1}{4\pi^2} P.V. \int_{-\pi}^{\pi} \int_{-\pi}^{\pi} \hat{v}(x, y) e^{-i(xm + yn)} dx dy$$

can be reduced to the single integral

$$v_{m,n} = v_- - \frac{1}{4\pi i} P.V. \int_{-\pi}^{\pi} \frac{\sin^2 \frac{\mu x}{2} e^{ix(m + \mu(n-1) - \frac{1}{2})}}{\sin \frac{x}{2} (\chi \sin^2 \frac{x}{2} + \sin^2 \frac{\mu x}{2})} dx.$$

Here the notation *P.V.* (principal value integral) is used because the integrand in (14) possesses a singularity at $x = 0$. To resolve the singularity, we deform the contour of integration in the complex plane so that the new contour Γ goes from $-\pi$ to π along the real axis everywhere except a small neighborhood near the origin, where it goes below the real axis (see Fig. 2). We thus obtain

$$v_{m,n} = v_- - \frac{1}{4\pi i} \int_{\Gamma} \frac{\sin^2 \frac{\mu x}{2} e^{ix\xi}}{\sin \frac{x}{2} (\chi \sin^2 \frac{x}{2} + \sin^2 \frac{\mu x}{2})} dx, \quad (14)$$

where we defined

$$\xi = m + \mu(n - 1) - \frac{1}{2}. \quad (15)$$

Notice that $\xi = 0$ is a straight line separating the vertical springs that are in phase I ($\xi > 0$) from the ones that are in phase II ($\xi < 0$). The integral in (14) can be evaluated using the residue theorem, closing the contour of integration by a rectangular contour of height R , $R \rightarrow \infty$, in the upper half-plane ($\text{Im } x > 0$) when $\xi > 0$ and lower half-plane otherwise, as shown in Fig. 2a. When μ is an even integer, the integrand in (14) has four symmetric poles with real parts equal to $\pm\pi$. By periodicity, we only need to include the pair of roots with real part equal π , so the vertical parts of the contour are deformed as shown in Fig. 2b. We can show that the contribution due to the vertical sides of the

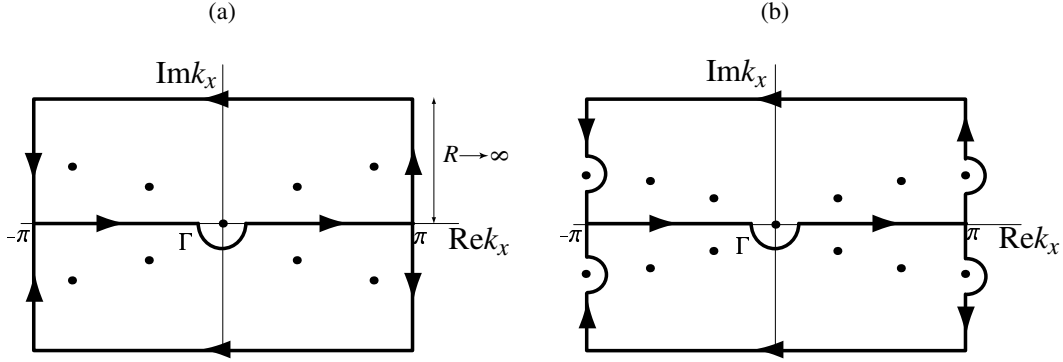


Figure 2: The contours of integration and the poles in the case of odd (a) and even (b) μ . The sets M_{\pm} are the nonzero poles inside the upper and lower closed contours.

rectangular contour cancel each other out. Meanwhile, the contribution due to the part of the contour parallel to the real axis tends to zero as the height R of the rectangle tends to infinity. For example, for $x = x + iR$, $-\pi \leq x \leq \pi$, with large R we have

$$\left| \frac{\sin^2 \frac{\mu x}{2} e^{ix\xi}}{\sin \frac{x}{2} (\chi \sin^2 \frac{x}{2} + \sin^2 \frac{\mu x}{2})} \right| \sim e^{-(\xi + \frac{1}{2})R} \rightarrow 0$$

as $R \rightarrow \infty$ for $\xi > 0$. Thus by residue theorem the value of the integral in (14) is determined by the sum of residues inside the closed contour. In addition to the simple pole at the origin, there is a finite number of complex poles (with nonzero real and imaginary parts) contained in the sets

$$M_{\pm} = \left\{ x : \sin^2 \frac{\mu x}{2} + \chi \sin^2 \frac{x}{2} = 0, \operatorname{Im} x \gtrless 0, -\pi < \operatorname{Re} x \leq \pi \right\}. \quad (16)$$

It is easy to see that the poles come in symmetric quadruples: if $x \in M_+$, then $-\bar{x} \in M_+$ and $-x, \bar{x} \in M_-$; see Fig. 2. The number of elements in M_{\pm} increases with μ . The imaginary parts of the poles tend to zero as μ tends to infinity or χ tends to zero.

In the degenerate case $\mu = 1$, the sets M_{\pm} are empty, and the solution has piecewise constant vertical strain:

$$v_{m,n} = \begin{cases} v_+, & \xi > 0, \\ v_-, & \xi < 0. \end{cases} \quad (17)$$

In the generic case when $1 < \mu < \infty$, the sets (16) contain at least two elements each, and the solution is given by

$$v_{m,n} = \begin{cases} v_+ - \sum_{x \in M_+} h(x) e^{ix\xi}, & \xi > 0, \\ v_- + \sum_{x \in M_-} h(x) e^{ix\xi}, & \xi < 0, \end{cases} \quad (18)$$

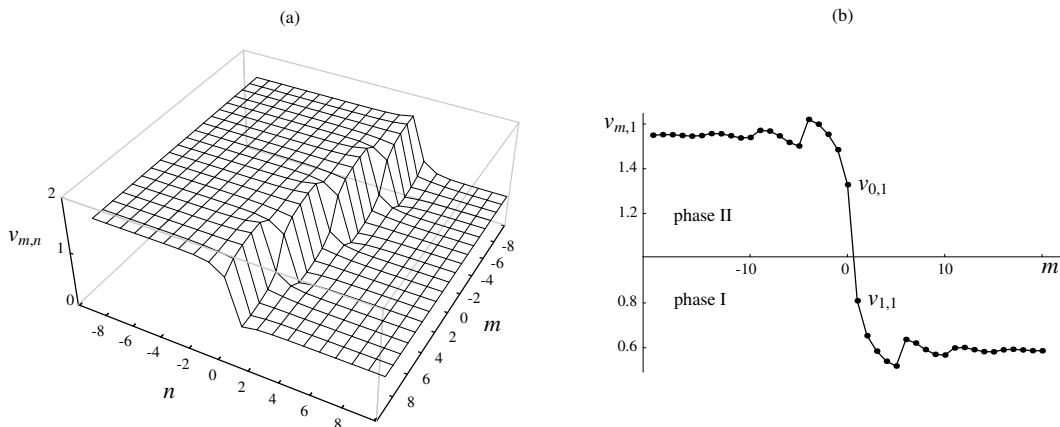


Figure 3: (a) A typical solution for vertical strain $v_{m,n}$ in the case of periodic steps with an integer period; (b) the strain profile along the line $n = 1$. Here $\mu = 5$, $v_- = 1.55$, $v_c = 1$ and $\chi = 1$.

with

$$h(x) = \frac{\sin^2 \frac{\mu x}{2}}{\sin \frac{x}{2} (\mu \sin \mu x + \chi \sin x)}. \quad (19)$$

In both (17) and (18) ξ is given by (15) and the vertical strains at infinity are related by

$$v_+ = v_- - \frac{\mu^2}{\mu^2 + \chi}. \quad (20)$$

A typical graph of vertical strain is shown in Figure 3a. As expected, solution is periodic, with period 1 in n -direction and period μ in m -direction. We see that unlike the cases $\mu = 1$ and $\mu = \infty$, the strain is no longer piecewise constant. Instead, there are now boundary layers near the phase boundary. In particular, the strain profile at each fixed n is monotonically decreasing in a transition layer around the phase boundary (see Figure 3b), due to the imaginary parts of the roots contained in M_{\pm} . The real parts of these roots contribute to oscillations outside the transition layer. The amplitude of these oscillations rapidly decays, and the strain reaches the constant values v_{\pm} as $m \rightarrow \pm\infty$.

For consistency with our assumptions we must also require that all vertical springs located at or below the phase boundary ($\xi < 0$) are in phase II, while the rest are in phase I:

$$v_{m,n} > v_c \text{ for } \xi < 0 \quad \text{and} \quad v_{m,n} < v_c \text{ for } \xi > 0. \quad (21)$$

This gives bounds on v_- and hence on the vertical component of the applied stress. Due to the monotone structure of the solution around the phase boundary for each fixed n ,

the first vertical springs to violate (21) are the ones on and directly in front of a step. Indeed, consider for example the strain profile along $n = 1$ shown in Figure 3b. As v_- is increased, the first strain to reach the critical value $v_c = 1$ is $v_{1,1}$, in the vertical spring just in front of the step. Similarly, as we decrease the applied strain, the strain $v_{0,1}$ in the vertical spring along the step reaches the critical value first. But the strain is periodic, so the strain profile at any fixed n is a translated version (by an integer multiple of μ) of the one just considered. This suggests that the constraints (21) are satisfied whenever

$$v_{1,1} < v_c, \quad v_{0,1} > v_c. \quad (22)$$

Hence the constructed solution exists, whenever the applied strain stays within the bounds $v_-^l < v_- < v_-^u$, where the lower and upper bounds are given by

$$v_-^l = v_c - S, \quad v_-^u = v_c + \frac{\mu^2}{\mu^2 + \chi} + S, \quad (23)$$

with

$$S = \sum_{x \in M_+} h(x) \exp(ix/2). \quad (24)$$

The upper bound $v_- = v_-^u$ corresponds to the springs just in front of each step reaching the critical strain, ready to switch to phase II. Meanwhile, the lower bound indicates that the springs along the steps are about to change phase back to phase I if v_- is further decreased.

To complete solution we also need to find the strains in the horizontal springs. As before, we only need to consider the case $1 \leq \mu < \infty$. Let

$$u_{m,n} = w_{m,n} - w_{m-1,n}$$

denote the horizontal strains. Using (6) and periodicity of the phase boundary, we obtain the equilibrium equation in terms of $u_{m,n}$ only:

$$\begin{aligned} & \chi(u_{m+1,n} + u_{m-1,n} - 2u_{m,n}) + (u_{m,n+1} + u_{m,n-1} - 2u_{m,n}) \\ &= - \sum_p \sum_{l=1}^{\mu} (\delta_{m,l-p\mu} - \delta_{m-1,l-p\mu}) \delta_{n,p}. \end{aligned}$$

This equation can again be solved by Fourier transform. We obtain

$$u_{m,n} = u_- - \frac{1}{4\pi i} P.V. \int_{-\pi}^{\pi} \frac{\sin \frac{\mu x}{2} e^{ix\eta}}{\chi \sin^2 \frac{x}{2} + \sin^2 \frac{\mu x}{2}} dx, \quad (25)$$

where

$$\eta = m + \mu \left(n - \frac{1}{2}\right) - 1 \quad (26)$$

and we assumed that the horizontal strains tend to constant values at infinities: $u_{m,n} \rightarrow u_{\pm}$. As in the case of vertical strains, the integral in (25) can be evaluated using the residue theorem. We find that in the case $\mu = 1$ the horizontal strains are piecewise constant:

$$u_{m,n} = \begin{cases} u_+, & \eta > 0, \\ u_-, & \eta < 0, \end{cases} \quad (27)$$

while in the generic case $1 < \mu < \infty$ we have

$$u_{m,n} = \begin{cases} u_+ - \sum_{x \in M_+} g(x) e^{ix\eta}, & \eta > 0, \\ u_- + \sum_{x \in M_-} g(x) e^{ix\eta}, & \eta < 0, \end{cases} \quad (28)$$

with

$$g(x) = \frac{\sin \frac{\mu x}{2}}{\mu \sin \mu x + \chi \sin x}. \quad (29)$$

In both cases the horizontal strains at infinity are related by

$$u_+ = u_- - \frac{\mu}{\mu^2 + \chi}. \quad (30)$$

Having solved the equations of equilibrium for horizontal and vertical strains that are derived from the equations (6) for displacement, we need to show that these solutions are compatible. Since the difference equations are linear, it suffices to show that the boundary conditions for the strains are compatible. In view of (20) and (30), we need to prove that the horizontal strains and vertical strains at infinity are related by

$$v_+ - v_- = -\frac{1}{1 + \chi/\mu^2} = \mu(u_+ - u_-). \quad (31)$$

The proof is presented in Appendix A.

4 Phase boundary with a periodic array of steps: rational slope

In the previous section we considered the case when the length of each step equals the period of the array, and the slope of the phase boundary is thus an integer. We now consider a more general situation where the array of steps is still periodic but each periodic cell may contain steps of variable length, so that the slope of the phase boundary is a rational number. An example of such periodic arrangement of steps is shown in Fig. 4, where the slope is $\mu = \frac{5}{2}$. In this case each periodic cell contains steps of length 2 and 3.

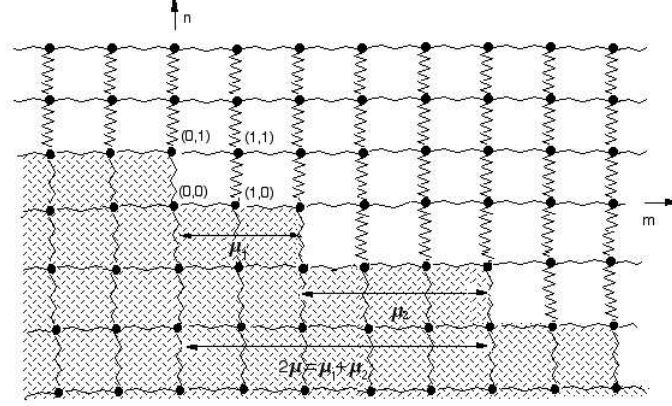


Figure 4: Periodic steps with a rational slope μ . Here $\mu = \frac{5}{2}$.

Let $\mu = r/s$ with $r, s \in \mathbb{Z} \setminus \{0\}$ be the rational slope of the phase boundary and let $\mu_j \in \mathbb{Z}$, $j = 1, \dots, s$, denote the length of j th step within one period. Clearly,

$$\mu = \frac{1}{s} \sum_{j=1}^s \mu_j.$$

The equations of equilibrium for the displacements $w_{m,n}$ are

$$\begin{aligned} & \chi(w_{m+1,n} + w_{m-1,n} - 2w_{m,n}) + (w_{m,n+1} + w_{m,n-1} - 2w_{m,n}) \\ &= - \sum_p \sum_{j=1}^s \sum_{l=1}^{\mu_j} \delta_{m,l-pr+\mu_1+\dots+\mu_{j-1}} \delta_{n,ps-j+1}. \end{aligned} \quad (32)$$

Hence for the vertical strains we obtain

$$\begin{aligned} & \chi(v_{m+1,n} + v_{m-1,n} - 2v_{m,n}) + (v_{m,n+1} + v_{m,n-1} - 2v_{m,n}) \\ &= - \sum_p \sum_{j=1}^s \sum_{l=1}^{\mu_j} \delta_{m,l-pr+\mu_1+\dots+\mu_{j-1}} (\delta_{n,ps-j+1} - \delta_{n-1,ps-j+1}). \end{aligned}$$

Discrete Fourier transform (12) of both sides in the above equation yields

$$\hat{v}(x, y) = \frac{\pi \sum_q \delta(sy - rx - 2\pi q)(1 - e^{iy})}{2(1 - e^{-ix})(\chi \sin^2 \frac{x}{2} + \sin^2 \frac{y}{2})} \sum_{j=1}^s e^{-i(j-1)y} e^{ix \sum_{t=0}^{j-1} \mu_t} (e^{i\mu_j x} - 1),$$

where we again used the identity (13). Observing that

$$\sum_q \delta(sy - rx - 2\pi q) = \sum_q \sum_{p=1}^s \delta(s(y - \mu x - 2\pi p/s - 2\pi q))$$

and applying inverse Fourier transform, we obtain

$$v_{m,n} = v_- - \frac{1}{4\pi i s} \sum_{p,j=1}^s \int_{\Gamma} \frac{\sin(\frac{\mu x}{2} - \frac{\pi p}{s}) \sin \frac{\mu_j x}{2} e^{i(x\xi_j + \alpha_{j,p})}}{\sin \frac{x}{2} (\chi \sin^2 \frac{x}{2} + \sin^2(\frac{\mu x}{2} - \frac{\pi p}{s}))} dx.$$

Here we defined

$$\xi_j = \xi + j\mu - \sum_{k=1}^j \mu_k + \frac{\mu_j - \mu}{2}, \quad (33)$$

where ξ is given in (15), and

$$\alpha_{j,p} = (3 - 2j - 2n)\pi p/s; \quad (34)$$

as before, the contour Γ goes along the segment $[-\pi, \pi]$ of the real axis except a small neighborhood near the origin, where it goes below the real axis. Applying the residue theorem to evaluate the above integral, we obtain

$$v_{m,n} = v_- - \sum_{j=1}^s \begin{cases} \frac{\mu \mu_j}{s(\mu^2 + \chi)} + \sum_{p=1}^s \sum_{x \in M_{+,p}} h_{j,p}(x) e^{ix\xi_j}, & \xi_j > 0, \\ - \sum_{p=1}^s \sum_{x \in M_{-,p}} h_{j,p}(x) e^{ix\xi_j}, & \xi_j < 0. \end{cases} \quad (35)$$

Here ξ_j are defined in (33),

$$M_{\pm,p} = \{x : \sin^2\left(\frac{\mu x}{2} - \frac{\pi p}{s}\right) + \chi \sin^2 \frac{x}{2} = 0, \text{ Im } x \geq 0, -\pi < \text{Re } x \leq \pi\} \quad (36)$$

denote the sets of poles for $p = 1, \dots, s$, and

$$h_{j,p}(x) = \frac{\sin(\mu \frac{x}{2} - \pi p/s) \sin \mu_j \frac{x}{2}}{s \sin \frac{x}{2} (\mu \sin(\mu x - 2\pi p/s) + \chi \sin x)} e^{i\alpha_{j,p}}$$

with $\alpha_{j,p}$ defined in (34) above. Observe that the strains far away above the phase boundary ($\xi_j > 0$, $j = 1, \dots, s$) tend to the constant strain v_+ given by

$$v_+ = v_- - \frac{\mu \sum_{j=1}^s \mu_j}{s(\chi + \mu^2)} = v_- - \frac{\mu^2}{\chi + \mu^2},$$

so that as in the periodic solution with integer period, the vertical strains at infinity are related by (20). In the special case of integer period ($s = 1$, $\mu_1 = \mu$), the above solution (35) reduces to the solution (18) we obtained in the previous section, with $\xi_j = \xi$ given in (15), $h_{1,1}(x) = h(x)$ defined in (19) and $M_{\pm,1} = M_{\pm}$ as in (16).

For the horizontal strains $u_{m,n}$ the equilibrium equations are

$$\begin{aligned} & \chi(u_{m+1,n} + u_{m-1,n} - 2u_{m,n}) + (u_{m,n+1} + u_{m,n-1} - 2u_{m,n}) \\ &= - \sum_p \sum_{j=1}^s \sum_{l=1}^{\mu_j} (\delta_{m,l-pr+\mu_1+\dots+\mu_{j-1}} - \delta_{m-1,l-pr+\mu_1+\dots+\mu_{j-1}}) \delta_{n,ps-(j-1)}. \end{aligned}$$

Solving this equation by Fourier transform, we obtain

$$u_{m,n} = u_- - \sum_{j=1}^s \begin{cases} \frac{\mu_j}{s(\mu^2+\chi)} + \sum_{p=1}^s \sum_{x \in M_{+,p}} g_{j,p}(x) e^{ix\eta_j}, & \eta_j > 0, \\ - \sum_{p=1}^s \sum_{x \in M_{-,p}} g_{j,p}(x) e^{ix\eta_j}, & \eta_j < 0. \end{cases} \quad (37)$$

Here

$$\eta_j = \eta + j\mu - \sum_{k=1}^j \mu_k + \frac{\mu_j - \mu}{2},$$

where η is given by (26), and

$$g_{j,p}(x) = \frac{\sin(\mu_j \frac{x}{2})}{s(\mu \sin(\mu x - 2\pi p/s) + \chi \sin x)} e^{2\pi p(1-j-n)/s}.$$

We can see that the strains u_{\pm} at infinity are related by (30), and the solution reduces to (28) in the special case $s = 1$.

As before, we need to impose the constraint that all vertical strains above (below) the phase boundary are in phase I (II). In addition, the equation of compatibility (31) can be proved in the same manner as for integer μ .

5 Equilibria with a non-periodic array of steps

The periodic solutions constructed in the previous sections exist only in a certain range of the applied strain, $v_-^l < v_- < v_-^u$. For example, in case of integer period the lower and upper bounds are given by (23). At the upper bound $v_- = v_-^u$, vertical springs in front of each step reach the critical strain v_c . If all of these springs transform to phase II at once, the whole phase boundary will move forward perpendicular to itself, and the solutions will transform to another periodic equilibrium. However, this scenario appears unlikely since it requires an infinite number of springs to transform at once. Another possibility

is that only a finite number of springs change phase. In this case the transformation will result in a non-periodic equilibrium that differs from the initial periodic state by a local perturbation. For example, in Fig. 5 a non-periodic state results from the phase change in the (1,1)th vertical spring directly in front of a step. In this section we will show how

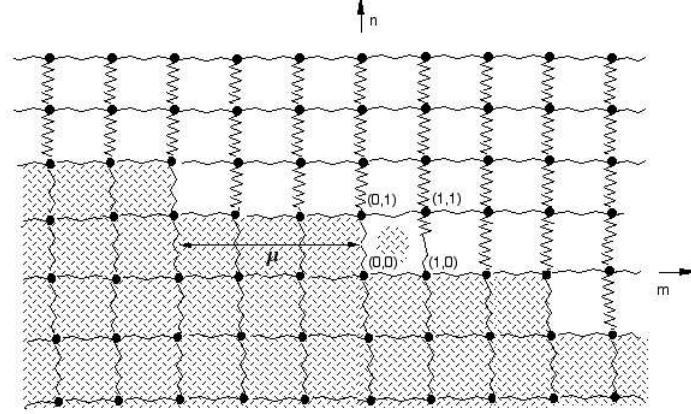


Figure 5: Transition from a periodic to a non-periodic equilibrium via transformation of a vertical spring in front of a step.

such equilibrium configurations can be calculated.

Consider first an equilibrium state obtained by transforming (p, q) th vertical spring *adjacent* to a periodic phase boundary. We assume that in the initial state the phase boundary has a rational slope, which includes the integer case. Equilibrium equations for displacement then read

$$\begin{aligned} & \chi(w_{m+1,n} + w_{m-1,n} - 2w_{m,n}) + (w_{m,n+1} + w_{m,n-1} - 2w_{m,n}) \\ &= - \sum_k \sum_{j=1}^s \sum_{l=1}^{\mu_j} \delta_{m,l-kr+\mu_1+\dots+\mu_{j-1}} \delta_{n,ks-j+1} + \delta_{m,p}(\delta_{n,q-1} - \delta_{n,q}). \end{aligned} \quad (38)$$

We can see that the first term in the right hand side of (38) is the same as in the periodic problem (32), with the additional term due to the transformed spring. By linear superposition, the vertical and horizontal strains for the non-periodic state under consideration can be written as

$$v_{m,n} = v_{m,n}^P + V_{m,n;p,q}, \quad u_{m,n} = u_{m,n}^P + U_{m,n;p,q}, \quad (39)$$

where $v_{m,n}^P$ and $u_{m,n}^P$ denote the solutions (35) and (37) obtained previously for vertical and horizontal strains in a periodic equilibrium, and the additional components $V_{m,n;p,q}$ and $U_{m,n;p,q}$ satisfy the equations

$$\begin{aligned} & \chi(V_{m+1,n} + V_{m-1,n} - 2V_{m,n}) + (V_{m,n+1} + V_{m,n-1} - 2V_{m,n}) \\ & = \delta_{m,p}(\delta_{n,q-1} - 2\delta_{n,q} + \delta_{n,q+1}). \end{aligned}$$

and

$$\begin{aligned} & \chi(U_{m+1,n} + U_{m-1,n} - 2U_{m,n}) + (U_{m,n+1} + U_{m,n-1} - 2U_{m,n}) \\ & = (\delta_{m,p} - \delta_{m,p+1})(\delta_{n,q-1} - \delta_{n,q}), \end{aligned}$$

respectively (for brevity, we omitted the indices p, q in the left hand side). Since the total strains $v_{m,n}$, $u_{m,n}$ satisfy the same conditions at infinity as the periodic components, we must also require that $V_{m,n;p,q}$, $U_{m,n;p,q} \rightarrow 0$ as $m, n \rightarrow \pm\infty$. Applying Fourier transform, we obtain

$$V_{m,n;p,q} = \frac{1}{\pi^2} \int_{0+}^{\pi} \int_{0+}^{\pi} \frac{\cos(p-m)x \cos(q-n)y \sin^2 \frac{y}{2}}{\chi \sin^2 \frac{x}{2} + \sin^2 \frac{y}{2}} dx dy \quad (40)$$

and

$$U_{m,n;p,q} = -\frac{1}{\pi^2} \int_{0+}^{\pi} \int_{0+}^{\pi} \frac{\sin(p+\frac{1}{2}-m)x \sin(q-\frac{1}{2}-n)y \sin \frac{y}{2} \sin \frac{3x}{2}}{\chi \sin^2 \frac{x}{2} + \sin^2 \frac{y}{2}} dx dy; \quad (41)$$

here and in what follows $0+$ in the integral limit denotes the zero limit from above. The functions $U_{m,n;p,q}$ and $V_{m,n;p,q}$ are Green's functions that can be used to construct solutions when a phase change occurs in a bond adjacent to a phase boundary.

The complete solution for a non-periodic equilibrium that differs by one spring from the periodic state is then given by (39), (35), (37), (40) and (41). In addition we need to require that the vertical strains stay in their respective phases on either side of the phase boundary. This constraint will result in bounds for v_- . Clearly, we can also obtain solutions with phase boundaries that differ from periodic by any number of springs, adjacent to the phase boundary, by superimposing the corresponding local perturbations $V_{m,n;p,q}$ and $U_{m,n;p,q}$.

As a simple example of a non-periodic equilibrium, consider the state obtained by transforming (1,1) vertical spring ($p = q = 1$) in front of a step of a periodic phase boundary with an integer slope, as shown in Fig. 5. In the resulting equilibrium state all steps are of length μ except two adjacent steps that are of length $\mu + 1$ and $\mu - 1$, respectively. The graph of vertical strain is shown in Fig. 6. Similar to the periodic case, for each fixed n the solution is monotonically decreasing inside a transition layer around the phase boundary. In view of the monotonicity, in order to find bounds on v_- it suffices

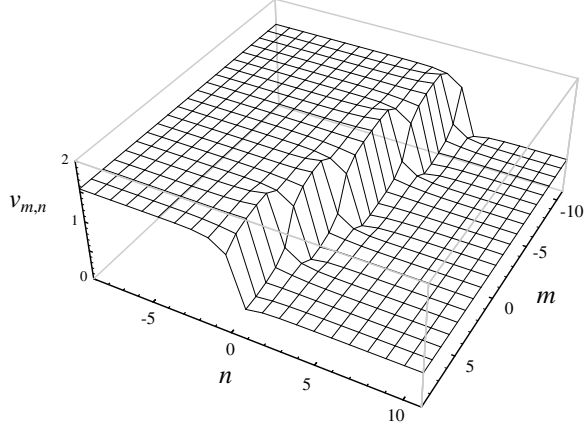


Figure 6: Typical solution for the vertical strain in the non-periodic equilibrium with $(1, 1)$ spring in phase II. Here $\mu = 5$, $v_- = 1.55$ and $\chi = 1$.

to require that the vertical springs directly in front and along each step are in phase I and II, respectively. In other words, we must require that

$$\max_p v_p^f < v_c, \quad \min_p v_p^a > v_c,$$

where $v_p^f = v_{\mu p+1, 1-p}$, $p \neq 0$, $v_0^f = v_{2,1}$ are the strains in vertical springs just in front of p th step, and $v_p^a = v_{\mu p, 1-p}$, $p \neq 0$, $v_0^a = v_{1,1}$ are the strains in springs along each step. For example, suppose that we start increasing the applied strain v_- . Recall that in the periodic solution this eventually leads to all vertical springs directly in front of the steps reaching critical strain v_c first. In the present case, due to a break in periodicity, there is a preference among these springs: namely, the strains in the springs behind and in front of the longer step, $v_1^f = v_{\mu+1, 0}$ and $v_{-1}^f = v_{-\mu+1, 2}$, are the largest and thus will reach v_c first as we increase v_- . Similarly, as we decrease v_- comparison of strain in vertical springs just behind the phase boundary shows that the strain $v_0^a = v_{1,1}$ is significantly smaller than the others and hence will reach the critical value first. See Fig. 7. Thus in order for this non-periodic equilibrium state to exist, the applied strain must be in the interval

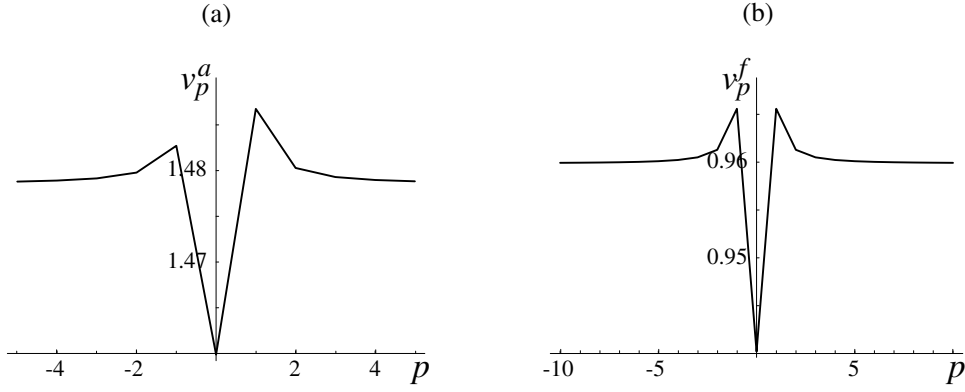


Figure 7: The strains along (a) and in front (b) of p th step along the phase boundary in the non-periodic equilibrium with $(1, 1)$ spring in phase II. Here $\mu = 5$, $v_- = 1.55$, $v_c = 1$ and $\chi = 1$.

$v_-^l < v < v_-^u$, where the upper and lower bounds are given by

$$\begin{aligned}
 v_-^u &= v_c + \frac{\mu^2}{\chi + \mu^2} + S \\
 &+ \frac{1}{\pi} \int_0^\pi \frac{\cos(\mu x) dx}{(1 + 2\chi \sin^2(\frac{x}{2}))[(1 + (1/\chi) \operatorname{cosec}^2(\frac{x}{2}))^{\frac{1}{2}} + 1]} + 1 \\
 v_-^l &= v_c + \frac{\mu^2}{\chi + \mu^2} + S - \frac{2}{\pi} \arctan \frac{1}{\sqrt{\chi}},
 \end{aligned}$$

where S is defined in (24).

6 Minimal barrier path between periodic and non-periodic arrays of steps

Consider an equilibrium with a periodic array of steps at a given applied force, or, equivalently, given v_- . For simplicity, we may assume that the period is an integer. Suppose now that at the same v_- there exists a non-periodic equilibrium which can be obtained from the periodic one by changing phase in a vertical spring in front of a step, as shown in Fig. 5. For instance, assume that in the non-periodic state the strain $v_{1,1} = w_{1,1} - w_{1,0}$ has changed phase. It is not hard to see that both equilibria are stable, in the sense that each is a local minimum of total energy, since in each state the strains are inside their respective energy wells. If the non-periodic equilibrium has less energy than the periodic one

(at a given applied force), the system may prefer to switch from periodic to non-periodic state. In order to do so, it has to follow a non-equilibrium path in the energy landscape that connects two local energy minima and goes through an energy barrier separating the two states.

Following similar constructions in [5] and [13] for a one-dimensional bi-stable chain, we can obtain a *minimal barrier path* from the periodic state to the non-periodic one by observing that along the path only $(1, 1)$ vertical spring changes phase, while the other vertical springs stay in their respective phases. The idea is then to minimize the energy along the path by performing the constrained minimization of the total energy at a given value of $v_{1,1}$. More precisely, we choose the *order parameter* $\alpha \in [0, 1]$ such that

$$v_{1,1} = \alpha v_{1,1}^{NP} + (1 - \alpha)v_{1,1}^P, \quad (42)$$

where $v_{m,n}^{NP}$ and $v_{m,n}^P$ denote the strains in periodic and non-periodic equilibria, respectively. Thus as α increases from 0 to 1 along the path, $v_{1,1}$ increases from $v_{1,1}^P < v_c$ ($\alpha = 0$) to $v_{1,1}^{NP} > v_c$ ($\alpha = 1$). We then minimize the total energy subject to the above constraint (42):

$$\min \{E(\{w_{m,n}\}_{m,n \in \mathbb{Z}}) + \lambda(w_{1,1} - w_{1,0} - \alpha v_{1,1}^{NP} - (1 - \alpha)v_{1,1}^P)\},$$

where $E = \sum_{m,n} (\phi_h(u_{m,n}) + \phi_v(v_{m,n}))$ is the total elastic energy of the system, and λ is the Lagrange multiplier due to the constraint. This results in the following equation for vertical strains:

$$\begin{aligned} & \chi(v_{m+1,n} + v_{m-1,n} - 2v_{m,n}) + (v_{m,n+1} + v_{m,n-1} - 2v_{m,n}) \\ & = \theta(v_{m,n+1} - v_c) - 2\theta(v_{m,n} - v_c) + \theta(v_{m,n-1} - v_c) \\ & - \lambda\delta_{m,1}(\delta_{n,0} - 2\delta_{n,1} + \delta_{n,2}). \end{aligned}$$

Observe that there exists $\alpha^* \in [0, 1)$ such that $v_{1,1}(\alpha^*) = v_c$. This value of the order parameter corresponds to the saddle point separating the two local minima in the energy landscape;¹ at this point the energy along the path is maximal. For $\alpha < \alpha^*$ we still have the periodic arrangement of steps (although clearly the strains are no longer periodic), whereas for $\alpha \geq \alpha^*$ the arrangement is necessarily non-periodic. Thus we obtain

$$\begin{aligned} & \chi(v_{m+1,n} + v_{m-1,n} - 2v_{m,n}) + (v_{m,n+1} + v_{m,n-1} - 2v_{m,n}) \\ & = - \sum_p \sum_{l=1}^{\mu} \delta_{m,l-p\mu} (\delta_{n,p} - \delta_{n-1,p}) \\ & + (\theta(\alpha - \alpha^*) - \lambda)\delta_{m,1}(\delta_{n,0} - 2\delta_{n,1} + \delta_{n,2}). \end{aligned}$$

¹Due to nonsmoothness of the energy in the bi-stable springs, $(1, 1)$ and $(1, 0)$ particles are in general *not* in equilibrium in the saddle-point configuration; indeed, observe that the Lagrange multiplier λ is nonzero at $\alpha = \alpha^*$ unless α^* equals zero.

Solving this equation and applying the constraint (42), we obtain

$$\lambda(\alpha) = \theta(\alpha - \alpha^*) - \alpha$$

and

$$v_{m,n}(\alpha) = v_{m,n}^P + \alpha V_{m,n},$$

where $V_{m,n} = V_{m,n;1,1}$ is the perturbation solution given by (40) with $p = q = 1$. Similarly, the horizontal strains along the path reduce to

$$u_{m,n}(\alpha) = u_{m,n}^P + \alpha U_{m,n},$$

with $U_{m,n} = U_{m,n;1,1}$ given in (41). Finally, we can find α^* by requiring that $v_{1,1}(\alpha^*) = v_c$. This yields

$$\alpha^* = \frac{1}{V_{1,1}}(v_c - v_{1,1}^P). \quad (43)$$

The free energy along the path is given by

$$\begin{aligned} G(\alpha) = & E(\alpha) - \sum_m ((\chi u_+ + v_+)w_{m,+\infty} - (\chi u_- + v_-)w_{m,-\infty}) \\ & - \sum_n ((\chi u_+ + v_+)w_{+\infty,n} - (\chi u_- + v_-)w_{-\infty,n}). \end{aligned}$$

Since this energy is infinite, we evaluate instead the difference between the free energy along the path and at the initial periodic equilibrium ($\alpha = 0$):

$$\begin{aligned} \Psi(\alpha) = & G(\alpha) - G(0) \\ = & E(\alpha) - E(0) - \alpha \sum_m ((\chi u_+ + v_+)W_{m,+\infty} - (\chi u_- + v_-)W_{m,-\infty}) \\ & - \alpha \sum_n ((\chi u_+ + v_+)W_{+\infty,n} - (\chi u_- + v_-)W_{-\infty,n}), \end{aligned}$$

where $W_{m,n}$ is the displacement due to the perturbation solution. But $W_{m,n}$ vanishes at points far from (1, 1), so that $W_{m,-\infty} = W_{-\infty,n} = 0$ and we obtain

$$\begin{aligned} \Psi(\alpha) = & E(\alpha) - E(0) = \sum_{m,n} \phi_h(u_{m,n}^P + \alpha U_{m,n}) - \sum_{m,n} \phi_h(u_{m,n}^P) \\ & + \sum_{m,n} \phi_v(v_{m,n}^P + \alpha V_{m,n}) - \sum_{m,n} \phi_v(v_{m,n}^P). \end{aligned}$$

Using (5), we obtain

$$\begin{aligned}\Psi(\alpha) = & \frac{1}{2} \left\{ \chi \sum_{m,n} (\alpha^2 U_{m,n}^2 + 2\alpha U_{m,n} u_{m,n}^P) + \sum_{m,n} (\alpha^2 V_{m,n}^2 + 2\alpha V_{m,n} v_{m,n}^P) \right\} \\ & - \sum_{m,n} (v_{m,n}^P - v_c) \{ \theta(v_{m,n}^P + \alpha V_{m,n} - v_c) - \theta(v_{m,n}^P - v_c) \} \\ & - \alpha \sum_{m,n} V_{m,n} \theta(v_{m,n}^P + \alpha V_{m,n} - v_c).\end{aligned}$$

Observe that in the last two terms we are summing only over the springs in the second phase. Recall that for $\alpha < \alpha^*$ the phase arrangement is the same as in the initial periodic state, i.e. $v_{m,n}^P + \alpha V_{m,n} > v_c$ for all m and n satisfying $m + \mu(n-1) < \frac{1}{2}$; for $\alpha > \alpha^*$ we also have $v_{1,1}^P + \alpha V_{1,1} \geq v_c$. Thus we obtain

$$\Psi(\alpha) = \frac{\alpha^2}{2} S_0 + \alpha S_1 - (v_{1,1}^P + \alpha V_{1,1} - v_c) \theta(\alpha - \alpha^*), \quad (44)$$

where

$$S_0 = \chi \sum_{m,n} U_{m,n}^2 + \sum_{m,n} V_{m,n}^2 \quad (45a)$$

$$S_1 = \chi \sum_{m,n} U_{m,n} u_{m,n}^P + \sum_{m,n} V_{m,n} v_{m,n}^P - \sum_n \sum_{m=-\infty}^{m_0(n)} V_{m,n}; \quad (45b)$$

in the last expression we set $m_0(n) = \lfloor 1/2 - \mu(n-1) \rfloor$. Finally, recall that Ψ must have local extrema at $\alpha = 0$ and $\alpha = 1$ since these are the states of equilibrium. Hence

$$\Psi'(0) = (\alpha S_0 + S_1)|_{\alpha=0} = 0 \quad (46a)$$

$$\Psi'(1) = (\alpha S_0 + S_1 - V_{1,1})|_{\alpha=1} = 0, \quad (46b)$$

which implies that $S_1 = 0$ and $S_0 = V_{1,1}$. Therefore the desired minimal barrier path is given by

$$\Psi(\alpha) = \frac{\alpha^2}{2} V_{1,1} - (v_{1,1}^P + \alpha V_{1,1} - v_c) \theta(\alpha - \alpha^*). \quad (47)$$

Here α^* is given in (43),

$$V_{1,1} = \frac{1}{\pi^2} \int_0^\pi \int_0^\pi \frac{\sin^2 \frac{y}{2}}{\chi \sin^2 \frac{x}{2} + \sin^2 \frac{y}{2}} dx dy = \frac{2}{\pi} \arctan \frac{1}{\sqrt{\chi}}$$

and

$$v_{1,1}^P = v_- - \frac{1}{1 + \chi/\mu^2} - S,$$

with S defined in (24).

We can now evaluate the energy barrier which is equal to the difference between the energies at the saddle point $\alpha = \alpha^*$ and the initial periodic state ($\alpha = 0$):

$$\Delta E = \Psi(\alpha^*) = \frac{(\alpha^*)^2}{2} V_{1,1} = \frac{2\pi}{\arctan(1/\sqrt{\chi})} \left(v_c - v_- + \frac{1}{1 + \chi/\mu^2} + S \right)^2.$$

The energy barrier is zero when the strain at infinity equals the upper bound, $v_- = v_-^u$, which is defined in (23). Following [13] and by analogy with dislocation theory, we will refer to the corresponding applied stress as the Peierls stress. Recall that at this stress all vertical springs in front of each step in the periodic equilibrium have reached the critical strain and thus can change phase with zero energy barrier. This Peierls state corresponds to the saddle-point equilibrium where $\alpha^* = 0$.

The energy barrier is maximal when the periodic and non-periodic states have the same energy: $\Psi(1) = \Psi(0) = 0$. This occurs when the applied stress equals to its Maxwell value, or $v_- = v_-^M$, where

$$v_-^M = v_-^u - \frac{1}{2} V_{1,1} = v_c + \frac{1}{1 + \chi/\mu^2} + S - \frac{1}{2\pi} \arctan \frac{1}{\chi},$$

and the energy barrier is

$$\Delta E_{max} = \frac{1}{4\pi} \arctan \frac{1}{\sqrt{\chi}}.$$

Note that the Maxwell energy barrier depends only on χ . For $v_- < v_-^M$ the periodic state has lower energy than the non-periodic one, and hence the transition to the non-periodic state is energetically unfavorable; instead, the reverse transition may take place.

7 Minimal barrier path in an energy landscape: a general order parameter

We can now generalize the construction of the minimal barrier path to the case when a finite number of springs change phase along the path, either simultaneously or in a sequence of transitions. We start with a periodic equilibrium with generally a rational period and assume that the vertical springs (p_i, q_i) , $i = 1, \dots, n_\alpha$ may change phase along the path which thus connects the periodic state to one or more neighboring non-periodic equilibria at the same value of the applied stress.

In this case we choose the *vector order parameter* $\boldsymbol{\alpha} = (\alpha_1, \dots, \alpha_{n_\alpha})$, $0 \leq \alpha_i \leq 1$ for $i = 1, \dots, n_\alpha$. The values $\boldsymbol{\alpha} = \mathbf{0}$ and $\boldsymbol{\alpha} = \mathbf{1}$ correspond to the initial periodic and final non-periodic equilibrium states, respectively; along the path, each component α_i of the

order parameters is either fixed at 0 or monotonically increases from 0 to 1. Minimizing the total elastic energy along the path subject to the constraints

$$v_{p_i, q_i} = \alpha_i v_{p_i, q_i} |_{\alpha_i=1} + (1 - \alpha_i) v_{p_i, q_i} |_{\alpha_i=0}, \quad i = 1, \dots, n_\alpha, \quad (48)$$

we obtain the following equation for vertical strains:

$$\begin{aligned} & \chi(v_{m+1, n} + v_{m-1, n} - 2v_{m, n}) + (v_{m, n+1} + v_{m, n-1} - 2v_{m, n}) \\ & = \theta(v_{m, n+1} - v_c) - 2\theta(v_{m, n} - v_c) + \theta(v_{m, n-1} - v_c) \\ & - \sum_{i=1}^{n_\alpha} \lambda_i \delta_{m, p_i} (\delta_{n, q_i-1} - 2\delta_{n, q_i} + \delta_{n, q_i+1}) \end{aligned}$$

with the Lagrange multipliers λ_i determined by the constraints (48).

Let the set σ_i be defined by

$$\sigma_i = \{\boldsymbol{\alpha} : v_{p_i, q_i}(\boldsymbol{\alpha}) > v_c\}, \quad (49)$$

i.e. $\boldsymbol{\alpha} \in \sigma_i$ whenever the (p_i, q_i) th vertical spring is in phase II, and let $|\boldsymbol{\alpha} - \sigma_i|$ denote the distance between $\boldsymbol{\alpha}$ and the set σ_i . Using this and the fact that the initial state is a periodic equilibrium, we obtain

$$\begin{aligned} & \chi(v_{m+1, n} + v_{m-1, n} - 2v_{m, n}) + (v_{m, n+1} + v_{m, n-1} - 2v_{m, n}) \\ & = - \sum_p \sum_{j=1}^s \sum_{l=1}^{\mu_j} \delta_{m, l-pr+\mu_1+\dots+\mu_{j-1}} \delta_{n, ps-j+1} \\ & + [\theta(-|\boldsymbol{\alpha} - \sigma_i|) - \lambda_i] \delta_{m, p_i} (\delta_{n, q_i-1} - 2\delta_{n, q_i} + \delta_{n, q_i+1}). \end{aligned}$$

Solving these equations and enforcing the constraints (48), we get

$$\lambda_i(\boldsymbol{\alpha}) = \theta(-|\boldsymbol{\alpha} - \sigma_i|) - \alpha_i$$

and

$$v_{m, n}(\boldsymbol{\alpha}) = v_{m, n}^P + \sum_{i=1}^{n_\alpha} \alpha_i V_{m, n; p_i, q_i}.$$

Similar calculations yield the horizontal strains

$$u_{m, n} = u_{m, n}^P + \sum_{i=1}^{n_\alpha} \alpha_i U_{m, n; p_i, q_i}.$$

Here $v_{m,n}^P$ and $u_{m,n}^P$ are the strains in the initial periodic equilibrium. The boundaries of the sets σ_i defined in (49) are given by the hyperplanes S_i that represent the higher-dimensional version of α^* introduced in the previous section. They are defined by

$$S_i = \{\boldsymbol{\alpha} : v_{p_i, q_i}^P + \sum_{j=1}^{n_\alpha} \alpha_j V_{p_i, q_i; p_j, q_j} = v_c\}.$$

Thus we have

$$\theta(-|\boldsymbol{\alpha} - \sigma_i|) = \theta(|\boldsymbol{\alpha} - S_i|) = \theta(v_{p_i, q_i}^P + \sum_{j=1}^{n_\alpha} \alpha_j V_{p_i, q_i; p_j, q_j} - v_c).$$

We now evaluate $\Psi(\boldsymbol{\alpha})$:

$$\begin{aligned} \Psi(\boldsymbol{\alpha}) &= \frac{\chi}{2} \sum_{m,n} (u_{m,n}^P + \sum_{i=1}^{n_\alpha} \alpha_i U_{m,n; p_i, q_i})^2 - \frac{\chi}{2} \sum_{m,n} (u_{m,n}^P)^2 \\ &\quad + \frac{1}{2} \sum_{m,n} (v_{m,n}^P + \sum_{i=1}^{n_\alpha} \alpha_i V_{m,n; p_i, q_i})^2 - \frac{1}{2} \sum_{m,n} (v_{m,n}^P)^2 \\ &\quad - \sum_{m,n} \left\{ (v_{m,n}^P + \sum_{j=1}^{n_\alpha} \alpha_j V_{m,n; p_j, q_j} - v_c) \theta(v_{m,n}^P + \sum_{j=1}^{n_\alpha} \alpha_j V_{m,n; p_j, q_j} - v_c) \right. \\ &\quad \left. - (v_{m,n}^P - v_c) \theta(v_{m,n}^P - v_c) \right\}. \end{aligned}$$

As in previous section, we can simplify this expression by observing that in the last two terms the sums are only over the vertical springs that are in second phase in the initial periodic state, plus the additional transformed springs (p_i, q_i) if $\boldsymbol{\alpha} \in \sigma_i$. Using this and the fact that $\Psi(\boldsymbol{\alpha})$ must have local extrema at any $\boldsymbol{\alpha}_0$ such that all its components are either zero or one, we obtain

$$\begin{aligned} \Psi(\boldsymbol{\alpha}) &= \frac{1}{2} \sum_{i=1}^{n_\alpha} \sum_{j=1}^{n_\alpha} \alpha_i V_{p_i, q_i; p_j, q_j} \alpha_j \\ &\quad - \sum_{i=1}^{n_\alpha} (v_{p_i, q_i}^P + \sum_{j=1}^{n_\alpha} \alpha_j V_{p_i, q_i; p_j, q_j} - v_c) \theta(v_{p_i, q_i}^P + \sum_{j=1}^{n_\alpha} \alpha_j V_{p_i, q_i; p_j, q_j} - v_c). \end{aligned}$$

It is convenient to rewrite the above expression in vector form. Let $\{\mathbf{e}_i\}_{i=1}^{n_\alpha}$ denote a unit orthonormal basis of \mathbb{R}^{n_α} so that $\boldsymbol{\alpha}$ can be represented as $\boldsymbol{\alpha} = \sum_{i=1}^{n_\alpha} \alpha_i \mathbf{e}_i$. Let \mathbf{V} denote a tensor second order tensor for \mathbb{R}^{n_α} so that $\mathbf{V} = \sum_{i=1}^{n_\alpha} \sum_{j=1}^{n_\alpha} V_{ij} \mathbf{e}_i \otimes \mathbf{e}_j$ with $V_{ij} = V_{p_i, q_i; p_j, q_j}$. Then the expression for Ψ can be written as

$$\Psi(\boldsymbol{\alpha}) = \frac{1}{2} \boldsymbol{\alpha} \cdot \mathbf{V} \boldsymbol{\alpha} - \sum_{i=1}^{n_\alpha} (v_{p_i, q_i}^P + \mathbf{e}_i \cdot \mathbf{V} \boldsymbol{\alpha} - v_c) \theta(v_{p_i, q_i}^P + \mathbf{e}_i \cdot \mathbf{V} \boldsymbol{\alpha} - v_c). \quad (50)$$

Note that $\Psi(\boldsymbol{\alpha})$ represents a multidimensional energy landscape. This landscape is a projection that restricts the actual energy landscape (which involves an infinite number of equilibrium states) to several neighboring equilibria with different locations of steps. These stable equilibrium configurations are the local minima separated by the energy barriers. Various curves parametrized by $\boldsymbol{\alpha}$ describe paths in this landscape that connect the stable equilibria.

8 Sequential versus simultaneous propagation of steps

To explore the energy landscape constructed in the previous section and its implications for possible motion of the steps, we now consider two particular paths involving sequential and simultaneous propagation of a steps and compute the energy barriers along these paths. For simplicity, we consider a periodic equilibrium with integer slope μ . We assume that at the end of both paths under consideration a finite number n of springs just in front of the steps change phase. Without loss of generality, we set $(p_1, q_1) = (1, 1)$, so that $(p_j, q_j) = ((j-1)\mu + 1, 2-j)$, $j = 1, \dots, n$.

Along the first path the steps propagate *sequentially*. To apply the calculations from the previous section, we set the n -dimensional order parameter

$$\boldsymbol{\alpha}(t) = \begin{cases} (t, 0, 0, \dots, 0), & 0 \leq t \leq 1 \\ (1, t-1, 0, \dots, 0), & 1 \leq t \leq 2 \\ \dots\dots\dots \\ (1, \dots, 1, t-n+1), & n-1 \leq t \leq n. \end{cases} \quad (51)$$

Here $t \in [0, n]$ is the single order parameter along the path tuned so that at the (p_k, q_k) th spring changes phase at some $t_k^* \in [k-1, k]$. The above implies that for $t \in [k-1, k]$, $k = 1, \dots, n$, the j th component of $\boldsymbol{\alpha}(t)$ is given by

$$\alpha_j(t) = \begin{cases} 1, & j \leq k-1 \\ t-k+1, & j = k \\ 0, & j \geq k+1. \end{cases} \quad (52)$$

Using (50), (52) and the symmetry of tensor \mathbf{V} defined in the previous section, we obtain for $t \in [k-1, k]$

$$\begin{aligned} \Psi(t) = & \frac{1}{2}(t-k+1)^2 V_{k,k} - \frac{1}{2} \sum_{i=1}^{k-1} \sum_{j=1}^{k-1} V_{i,j} + (k-1)(v_c - v_{(k-1)\mu+1, 2-k}^P) \\ & - \theta(t-t_k^*) \left(v_{(k-1)\mu+1, 2-k}^P + \sum_{j=1}^{k-1} V_{k,j} + (t-k+1)V_{k,k} - v_c \right), \end{aligned}$$

where

$$t_k^* = k - 1 + \frac{v_c - v_{(k-1)\mu+1,2-k}^P - \sum_{j=1}^{k-1} V_{k,j}}{V_{k,k}},$$

if $k \geq 2$ and

$$\Psi(t) = \frac{1}{2}t^2V_{1,1} - \theta(t - t_1^*)(v_{1,1}^P + tV_{1,1} - v_c)$$

with

$$t_1^* = \frac{v_c - v_{1,1}^P}{V_{1,1}}$$

if $k = 1$. Thus, the energy barrier for (p_k, q_k) th spring to switch phase is

$$\Delta E_k = \Psi(t_k^*) - \Psi(k - 1) = \frac{1}{2V_{k,k}}(v_c - v_{(k-1)\mu+1,2-k}^P - \sum_{j=1}^{k-1} V_{k,j})^2 \quad (53)$$

for $k \geq 2$ and

$$\Delta E_1 = \Psi(t_1^*) - \Psi(0) = \frac{1}{2V_{1,1}}(v_c - v_{1,1}^P)^2. \quad (54)$$

We now recall that for the periodic equilibrium we have

$$v_{(k-1)\mu+1,2-k}^P = v_- - \frac{\mu^2}{\mu^2 + \chi} - S,$$

for all k , where S is given by (24). The components of tensor \mathbf{V} are given by

$$\begin{aligned} V_{i,j} &= V_{(i-1)\mu+1,2-i;(j-1)\mu+1,2-j} \\ &= \frac{1}{\pi^2} \int_0^\pi \int_0^\pi \frac{\cos[(j-i)\mu x] \cos[(j-i)y] \sin^2 \frac{y}{2}}{\chi \sin^2 \frac{x}{2} + \sin^2 \frac{y}{2}} dx dy. \end{aligned} \quad (55)$$

In particular,

$$V_{i,i} = V_{1,1} = \frac{1}{\pi^2} \int_0^\pi \int_0^\pi \frac{\sin^2 \frac{y}{2}}{\chi \sin^2 \frac{x}{2} + \sin^2 \frac{y}{2}} dx dy = \frac{2}{\pi} \arctan \frac{1}{\sqrt{\chi}}. \quad (56)$$

Let \mathbb{Z}^+ denote the set of positive (non-zero) integers. We define a sequence of functions $\{I_k\}_{k \in \mathbb{Z}^+}$ with

$$I_k(\mu, \chi) = -\frac{1}{\pi} \int_0^\pi \cos(k\mu x) \sqrt{\frac{\lambda - 1}{\lambda + 1}} (\lambda - \sqrt{\lambda^2 - 1})^k dx, \quad (57)$$

where

$$\lambda = 1 + 2\chi \sin^2 \frac{x}{2}. \quad (58)$$

As shown in Appendix B, the off-diagonal entries reduce to

$$V_{i,j} = I_{|j-i|}, \quad (59)$$

as $i \neq j$. It is also convenient to define a sequence of functions $\{J_k\}_{k \in \mathbb{Z}^+}$ with

$$J_k(\mu, \chi) \equiv \begin{cases} \sum_{j=1}^{k-1} V_{k,j}, & k \geq 2 \\ 0, & k = 1 \end{cases} \quad (60)$$

Using (57), we obtain, after some algebraic manipulations,

$$J_k(\mu, \chi) = -\frac{1}{\pi} \int_0^\pi \sqrt{\frac{\lambda-1}{\lambda+1}} \mathcal{K}_k(\lambda - \sqrt{\lambda^2-1}, \mu, x) dx, \quad (61)$$

where we defined

$$\mathcal{K}_k(b, \mu, x) \equiv \frac{b^k \cos(\mu k x) - b^{k+1} \cos(\mu(k-1)x) + b^2 - b \cos(\mu x)}{2b \cos(\mu x) - b^2 - 1} \quad (62)$$

for $k \geq 2$ and set $\mathcal{K}_1 \equiv 0$. Then the energy barriers (53), (54) are given by

$$\Delta E_k(\mu, \chi) = \frac{\pi}{4 \arctan(1/\sqrt{\chi})} \left(v_c - v_- + \frac{\mu^2}{\mu^2 + \chi} + S - J_k(\mu, \chi) \right)^2, \quad (63)$$

with $J_k(\mu, \chi)$ given by (61), (62).

The behavior of energy barriers is thus determined by the properties of functions in the set $\{I_k\}_{k \in \mathbb{Z}^+}$ that represent the off-diagonal entries of the tensor V by (57) and (59). The following proposition summarizes these properties:

Proposition 1:

- (a) $|\sum_{j=1}^k I_j| < \frac{1}{2} V_{1,1}$ for all $k \in \mathbb{Z}^+$.
- (b) The elements of the sequence $\{I_k\}_{k \in \mathbb{Z}^+}$ tend to zero as $k \rightarrow \infty$, monotonically at large k and $\chi \neq \mu^2$.
- (c) There exists a sequence of functions $\{\chi_k : \mathbb{Z} \rightarrow \mathbb{R}\}_{k \in \mathbb{Z}^+}$ such that for all $\mu, k \in \mathbb{Z}^+$, $I_k(\mu, \chi_k(\mu)) = 0$ and $I_k(\mu, \chi) > 0$ for $0 < \chi < \chi_k(\mu)$.

The proof of this proposition can be found in Appendix C. In addition, we state the following conjecture:

Conjecture: For each $k, \mu \in \mathbb{Z}^+$, $\chi_k(\mu)$ as defined in Proposition 1(c) is the unique positive root of $I_k(\mu, \chi) = 0$. The sequence $\{\chi_k(\mu)\}$ strictly monotonically increases with k and tends to μ^2 as $k \rightarrow \infty$.

Although we were unable to prove it, the conjecture is strongly supported by our numerical calculations; see, for example, Figure 8. Note also that the leading term in the

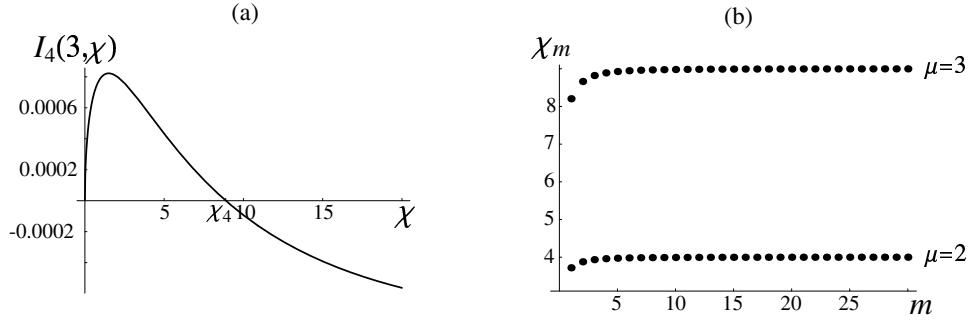


Figure 8: (a) The function $I_4(3, \chi)$ and (b) the sequence $\chi_k(\mu)$ at $\mu = 2$ and $\mu = 3$.

asymptotic expression (73) for I_k at large k vanishes at $\chi = \mu^2$, suggesting that this is the limit of the sequence. The conjecture immediately implies

Corollary:

(1) $I_k(\mu, \chi) > 0$ for all $k \in \mathbb{Z}^+$ when $\chi < \chi_1(\mu)$. When $\chi > \mu^2$, $I_k(\mu, \chi) < 0$ for all $k \in \mathbb{Z}^+$.

(2) For χ such that $\chi_1(\mu) \leq \chi \leq \mu^2$, we have $I_j(\mu, \chi) < 0$ for $j < k$, $I_k(\mu, \chi) \leq 0$, where k is such that $\chi_k(\mu) \leq \chi < \chi_{k+1}(\mu)$, and $I_j(\mu, \chi) > 0$ for $j > k$.

We can now use these results to obtain

Proposition 2:

(a) As $k \rightarrow \infty$, the energy barriers along the path approach the limiting value

$$\Delta E_\infty(\mu, \chi) \equiv \lim_{k \rightarrow \infty} \Delta E_k(\mu, \chi) = \frac{\pi}{4 \arctan(1/\sqrt{\chi})} \left\{ v_c - v_- + \frac{\mu^2}{\mu^2 + \chi} + S - \frac{\arctan \sqrt{\chi}}{\pi} - \chi \operatorname{Im} \left(\sum_{x \in M^+} \frac{\sin^2(\frac{x}{2})}{\mu \sin(\mu x) + \chi \sin x} \right) \right\}^2.$$

The limiting energy barrier is higher than the first energy barrier ($\Delta E_\infty(\mu, \chi) > \Delta E_1(\mu, \chi)$) if and only if $\chi > \chi_*(\mu)$, where $\chi_*(\mu)$ is the solution of the transcendental equation

$$\frac{\arctan \sqrt{\chi}}{\chi} - \pi \operatorname{Im} \left(\sum_{x \in M^+} \frac{\sin^2(\frac{x}{2})}{\mu \sin(\mu x) + \chi \sin x} \right) = 0, \quad (64)$$

and the two energy barriers are equal when $\chi = \chi_*(\mu)$.

(b) If $\chi < \chi_1(\mu)$, the energy barriers ΔE_k monotonically decrease to the limiting value ΔE_∞ . If $\chi > \mu^2$, the energy barriers monotonically increase to the limiting value. In the

intermediate range of χ , $\chi_1(\mu) \leq \chi \leq \mu^2$, the energy barriers ΔE_k increase for $k \leq k_*$ to reach the maximum energy barrier ΔE_{k_*} , where k_* is such that $\chi_{k_*-1}(\mu) \leq \chi < \chi_{k_*}(\mu)$, and monotonically decrease for $k > k_*$ to the limiting value.

The proof can be found in Appendix C. Note that Proposition 2 implies that the first energy barrier along the path exceeds the second ($\Delta E_1(\mu, \chi) > \Delta E_2(\mu, \chi)$) if and only if $\chi > \chi_1(\mu)$, where $\chi_1(\mu)$ solves the transcendental equation

$$\int_0^\pi \cos(\mu x) \sqrt{\frac{\lambda-1}{\lambda+1}} (\lambda - \sqrt{\lambda^2-1}) dx = 0 \quad (65)$$

with λ given by (58). The monotonicity for $\chi < \chi_1(\mu)$ implies that the first energy barrier is greater than the limiting one, so that $\chi_1(\mu) < \chi_*(\mu)$.

Figure 9 shows the threshold values $\chi_*(\mu)$, $\chi_1(\mu)$ at integer μ along with the graph of $\chi(\mu) = \mu^2$. We can see that $\chi_1(\mu) < \chi_*(\mu) < \mu^2$.

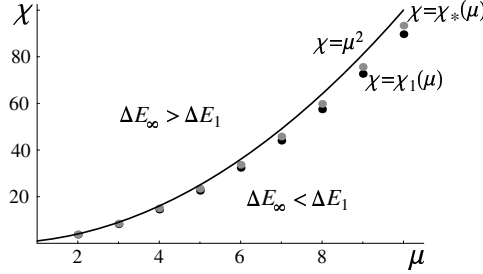


Figure 9: The threshold values $\chi_1(\mu)$ (black dots) and $\chi_*(\mu)$ (grey dots) at integer μ .

To illustrate the results of Proposition 2, we consider the case $\mu = 3$. In this case we have $\chi_1 = 8.20$ and $\chi_* = 8.49$. At $\chi = 7 < \chi_1$, the energy barriers ΔE_k monotonically decrease to ΔE_∞ for all k , so that the first energy barrier is the largest one, as shown in Fig. 10a. Thus if the system has enough energy H to overcome the first energy barrier ($H \geq \Delta E_1$), it can automatically overcome all other (smaller) energy barriers. So in this case climbing over the first energy barrier (moving one step) initiates a cascade motion of the other steps.

At χ in the intermediate range, $\chi_1 < \chi < \mu^2$, the first energy barrier is smaller than the second, and after reaching the maximum energy barrier, the energy barriers monotonically decrease to the limiting energy barrier satisfying $\Delta E_\infty < \Delta E_1$ if $\chi < \chi_*$ (see, for example, the case $\chi = 8.3$ in Fig. 10b) and $\Delta E_\infty > \Delta E_1$ if $\chi > \chi_*$ (e.g. $\chi = 8.71$ in Fig. 10c). In this case the maximum energy barrier along the path occurs at finite k (second barrier in Fig. 10b and third in Fig. 10c). If the amount H of energy in the system is less than this maximum energy barrier (but greater than the first), only several steps

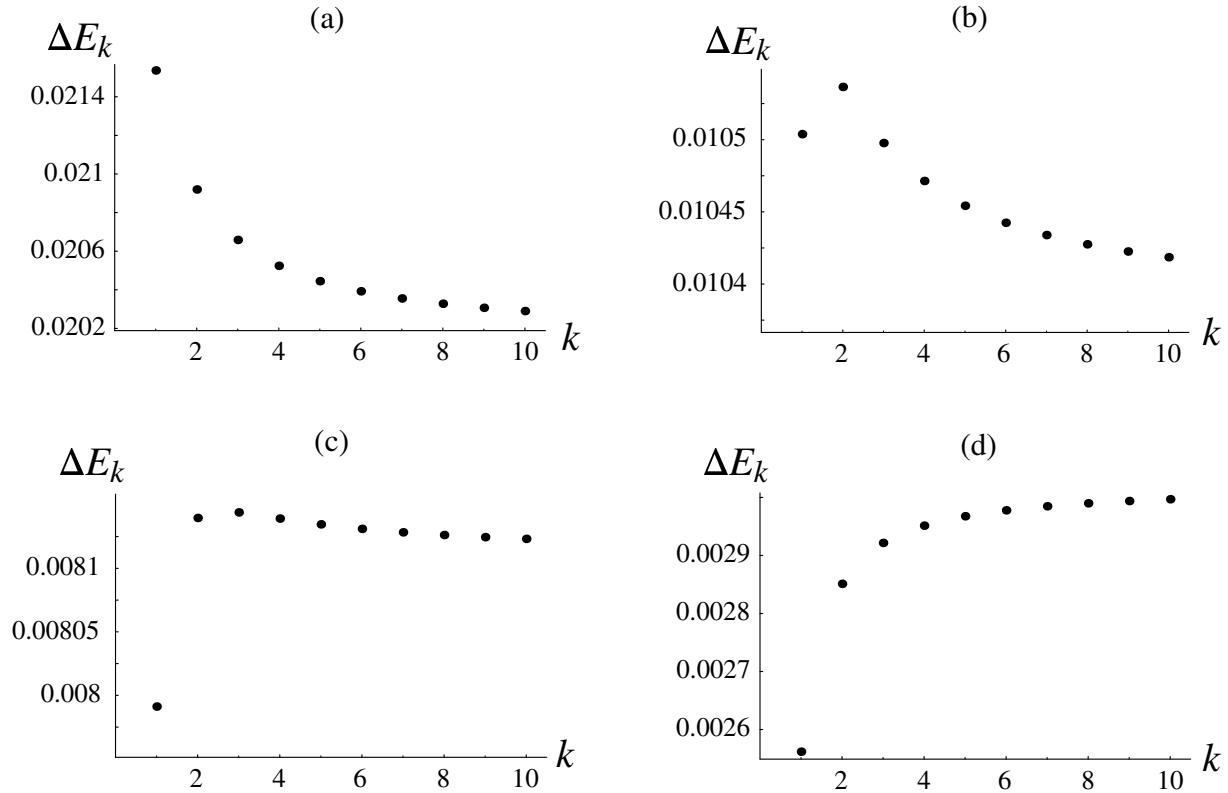


Figure 10: Energy barriers during sequential propagation of steps: (a) $\chi = 7$ ($\chi < \chi_1(\mu)$); (b) $\chi = 8.3$ ($\chi_1 < \chi < \chi_*$); (c) $\chi = 8.71$ ($\chi_* < \chi < \mu^2$); (d) $\chi = 10$ ($\chi > \mu^2$). In all cases $\mu = 3$, $v_c = 1$ and $v_- = 1.3$.

in the sequence will move. Physically, this means that on one hand, sufficiently strong horizontal bonds appear to be limiting the step motion. Note, however, that on the other hand, the maximum energy barrier along the path decreases with χ (at fixed v_-), so that less energy is needed to overcome it.

Finally, the case of large χ ($\chi = 10 > \mu^2$) is shown in Fig. 10d. In this case the energy barriers monotonically increase to the maximal limiting value for all k (recall that monotone increase at large k follows from the Proposition 1). As in the previous case, this leads to only several steps moving if H is less than the maximal energy barrier.

Now consider a path along which all n springs are allowed to change phase together. In this case the n -dimensional vector order parameter is given by

$$\boldsymbol{\alpha}(t) = \left(\frac{t}{n}, \frac{t}{n}, \dots, \frac{t}{n} \right),$$

with $t \in [0, n]$ as before. The energy (50) along this path reduces to

$$\Psi(t) = \frac{1}{2} \left(\frac{t}{n} \right)^2 \sum_{i=1}^n \sum_{j=1}^n V_{i,j} - \sum_{i=1}^n \left(v_{1,1}^P + \frac{t}{n} \sum_{j=1}^n V_{i,j} - v_c \right) \theta(t - t_i^*),$$

where we used periodicity of the initial equilibrium and defined

$$t_i^* = \frac{v_c - v_{1,1}^P}{\sum_{j=1}^n V_{i,j}} n$$

as the value of the parameter t at which (p_i, q_i) th and (p_{n-i+1}, q_{n-i+1}) springs change phase (so that $t_i^* = t_{n-i+1}^*$). Note that the two springs must necessarily change phase together along this path because

$$\sum_{j=1}^n V_{i,j} = \sum_{j=1}^n V_{n-i+1,j}.$$

This is true because of the special Toeplitz structure of the tensor \mathbf{V} : in the basis under consideration it is represented by a multidiagonal symmetric matrix with constant entries along each diagonal. Observe, however, that unless $n = 2$ the n springs under consideration do *not* change phase at the same value of t but rather do so in pairs at successive values $t = t_i^*$ for each pair. Thus the phase change along this path is not truly simultaneous unless $n = 2$.

To compute the energy barrier, we determine the *smallest* t_i^* :

$$t^* = \min_{1 \leq i \leq n} t_i^* = \frac{v_c - v_{1,1}^P}{\max_{1 \leq i \leq n} \sum_{j=1}^n V_{i,j}} n$$

and recall that $v_{1,1}^P = v_- - \frac{\mu^2}{\mu^2 + \chi} - S$. We then obtain

$$\Delta E = \Psi(t^*) = \frac{\sum_{i,j=1}^n V_{i,j}}{2 \left(\max_{1 \leq i \leq n} \sum_{j=1}^n V_{i,j} \right)^2} \left(v_c - v_- + \frac{\mu^2}{\mu^2 + \chi} + S \right)^2 \quad (66)$$

This is the energy barrier for the first pair of springs to switch phase but we can show that it is also the energy barrier for all n springs because the energy $\Psi(t)$ starts decreasing after the first pair of springs changes phase.

We can now compare the computed energy barrier for “simultaneous” phase change to the first energy barrier the system needs to overcome in order to initiate sequential step propagation. Recalling (63) and (56), we see that the latter is given by

$$\Delta E_1 = \frac{1}{2V_{1,1}} \left(v_c - v_- + \frac{\mu^2}{\mu^2 + \chi} + S \right)^2.$$

We now claim that for $n \geq 2$ the inequality $\Delta E > \Delta E_1$ always holds, i.e. the energy barrier (66) for “simultaneous” phase change is strictly greater than the first energy barrier for sequential propagation:

Proposition 3:

For $n \geq 2$,

$$\frac{\Delta E}{\Delta E_1} = \frac{V_{1,1} \sum_{i,j=1}^n V_{i,j}}{\left(\max_{1 \leq i \leq n} \sum_{j=1}^n V_{i,j} \right)^2} > 1.$$

The proof can be found in Appendix C.

9 Example: sequential versus simultaneous step propagation.

We start by considering the energy landscape that involves a periodic equilibrium with integer slope μ and nonperiodic states with either one or both vertical springs in front of two neighboring steps transformed to phase II. In this case $n_\alpha = 2$, $(p_1, q_1) = (1, 1)$ and $(p_2, q_2) = (\mu + 1, 0)$. Recall that

$$v_{\mu+1,0}^P = v_{1,1}^P = v_- - \frac{1}{1 + \chi/\mu^2} - S,$$

with S given in (24). Substituting this along with (56), (57) and (59) in (50), we obtain two-dimensional energy landscape $\Psi(\alpha_1, \alpha_2)$ an example of which is shown in Figure 11. Here the parameters μ and χ are chosen so that $\chi < \chi_1(\mu)$. As in the previous section, we now consider sequential (path 1) versus simultaneous (path 2) propagation of the two steps involved. Due to the symmetry of the landscape, it does not matter which of the two springs changes phase first along path 1: if the order is reversed, the energy profile is exactly the same. As already discussed, the energy barrier along the second path is almost twice as high as the first energy barrier along sequential propagation. See Figure 12. Moreover, the energy barrier ΔE along path 2 (simultaneous propagation) is strictly greater than the *sum* of energy barriers ΔE_1 and ΔE_2 along the (sequential) path 1: $\Delta E - \Delta E_1 - \Delta E_2 \approx 0.0013 > 0$. This is because the second energy barrier along path 1 is smaller than the first (as predicted for the case $\chi < \chi_1(\mu)$). These results suggest that sequential propagation of steps is energetically preferred.

Similarly, we can consider the case when four springs can transform ($n_\alpha = 4$): $(p_1, q_1) = (1, 1)$, $(p_2, q_2) = (\mu + 1, 0)$, $(p_3, q_3) = (2\mu + 1, -1)$ and $(p_4, q_4) = (3\mu + 1, -2)$. In this case the energy landscape $\Psi(\alpha_1, \alpha_2, \alpha_3, \alpha_4)$ is a four-dimensional surface that is hard to visualize. Instead, we again consider sequential (path 1) versus “simultaneous” (path

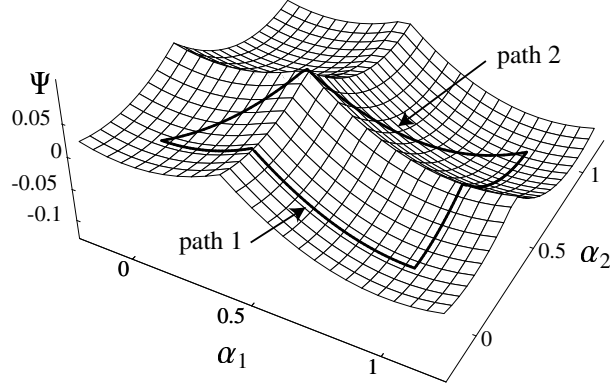


Figure 11: Energy landscape for connecting periodic equilibrium with integer slope to neighboring nonperiodic minimizers, with two springs changing phase. Along path 1 the two springs change phase sequentially. Path 2 corresponds two simultaneous phase change in the two springs. Parameters: $\mu = 5$, $v_- = 1.55$, $v_c = 1$ and $\chi = 1$.

2) propagation. As we recall from the previous section, the propagation is not truly simultaneous along the second path. Instead, two pairs of springs change phase one after another; for example, in the case considered here ($\mu = 5$, $\chi = 1$, $v_- = 1.55$), the two middle springs, (p_2, q_2) and (p_3, q_3) , change phase first at $t = t_1^* = 1.483$, and the other two springs change phase at $t = t_2^* = 1.498$.

Figure 13 compares the energy profiles along the two paths. The energy barrier $\Delta E = 0.14$ along path 2 is 3.9 times higher than the first energy barrier $\Delta E_1 = 0.036$ along the sequential path and is even larger than the sum of all energy barriers along path 1 which are slightly decreasing ($\Delta E_2 = 0.034$, $\Delta E_3 = 0.0335$, $\Delta E_4 = 0.0332$) since $\chi < \chi_1(\mu)$.

As we discussed above, in the case $\chi > \mu^2$ the energy barriers along the sequential path are slightly increasing. For example, in the case $\mu = 2$, $\chi = 5$, $v_- = 1.7$ and $v_c = 1$ we have $\Delta E_1 = 0.0165$, $\Delta E_2 = 0.0178$, $\Delta E_3 = 0.0182$ and $\Delta E_4 = 0.0184$ along path 1, while the energy barrier for path 2 is $\Delta E = 0.0669 \approx 4.05\Delta E_1$. So in this case the sequential path is again preferred, although the system may only move the first few steps if the energy barriers along the path become too high.

Finally, in the case $\chi_1(\mu) < \chi < \mu^2$, the maximum energy barrier along the sequential path is an interior one. For instance, at $\chi = 8.71$ and $\mu = 3$ (yielding $\chi_1 \approx 8.2$, $\chi_2 \approx 8.66$ and $\chi_3 \approx 8.82$, so that $\chi_2 < \chi < \chi_3$) we have $\Delta E_1 = 0.007991$, $\Delta E_2 = 0.008139$, $\Delta E_3 = 0.008144$ and $\Delta E_4 = 0.008139$ along path 1, so that the third energy barrier is slightly higher than others, as predicted by Proposition 2(b). Meanwhile, the energy barrier for path 2 is $\Delta E = 0.032 \approx 4.005\Delta E_1$. Note also that $\Delta E/\Delta E_3 \approx 3.93$, so that the energy barrier for path 2 is almost four times higher than the maximum energy barrier

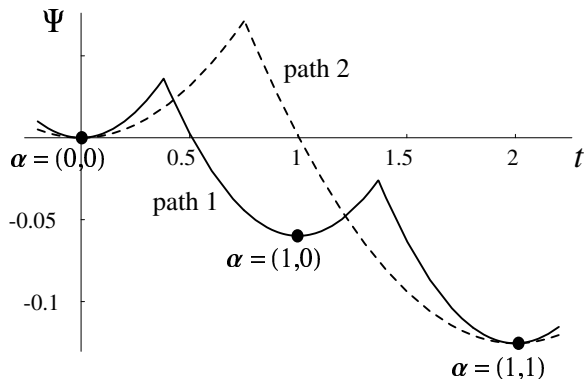


Figure 12: Sequential versus simultaneous propagation of two neighboring steps in a periodic equilibrium. Parameters: $\mu = 5$, $v_- = 1.55$, $v_c = 1$ and $\chi = 1$. Here $\chi < \chi_1(\mu)$.

along path 1. Hence if the system has enough energy to overcome the third energy barrier along path 1, sequential propagation would be energetically preferred.

10 Concluding remarks

In this paper we studied the quasistatic motion of steps along a phase boundary in a two-dimensional lattice model of phase transitions that incorporates material anisotropy. Assuming a bilinear interaction force in phase-transforming bonds, we constructed equilibria that contain a phase boundary with a rational slope as well as the neighboring non-periodic equilibria. Using a vector order parameter, we constructed minimal barrier paths connecting these equilibria and showed that the sequential motion of a finite number of steps requires a smaller energy barrier than simultaneous motion of the steps.

Our analysis shows that the size of energy barriers and the resulting step motion are significantly affected by material anisotropy parameter χ and the slope μ of the phase boundary. In particular, if χ is higher than a certain threshold (that increases with μ) step propagation may be prevented when the available energy to cause such motion is less than the largest energy barrier along the path, which, however, decreases as χ grows. Meanwhile, at smaller χ the motion of first step initiates the cascade motion in a sequential manner.

Although the analysis presented here relied on a number of modeling assumptions and simplifications in order to make the calculations as explicit as possible, our simple model contains the essential physics in order to illustrate the main features of quasistatic motion of a martensitic phase boundary. Future work will include deriving continuum formula-

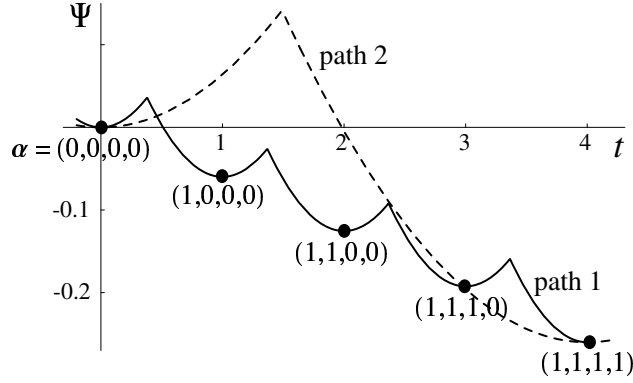


Figure 13: Sequential versus simultaneous propagation of four neighboring steps in a periodic equilibrium. Parameters: $\mu = 5$, $v_- = 1.55$, $v_c = 1$ and $\chi = 1$. Here $\chi < \chi_1(\mu)$.

tion that exhibits some of the results presented here, developing a numerical method to compute energy barriers for a fully nonlinear potential and conducting a comprehensive simulation of step motion under quasistatic loading.

Acknowledgements. This work was supported by the National Science Foundation grant DMS-0443928 (A.V.).

A Proof of compatibility condition

In this Appendix we prove the compatibility condition (31).

Let $m_0, n_0 \in \mathbb{Z}$ be such that $\xi_0 = m_0 + \mu(n_0 - 1) - 1/2 > 0$ and $m_0 + \mu(n_0 - 2) - 1/2 < 0$. Let $N > 0$ be an integer. Then

$$\sum_{n=n_0}^N v_{m_0,n} = \sum_{n=n_0}^N w_{m_0,n} - \sum_{n=n_0}^N w_{m_0,n-1} = w_{m_0,N} - w_{m_0,n_0-1}$$

so that $u_{m_0,N} = w_{m_0,N} - w_{m_0-1,N} = u_{m_0,n_0-1} + \sum_{n=n_0}^N (v_{m_0,n} - v_{m_0-1,n})$. Similarly, $u_{m_0,-N} = w_{m_0,-N} - w_{m_0-1,-N} = u_{m_0,n_0-1} - \sum_{n=-N+1}^{n_0-1} (v_{m_0,n} - v_{m_0-1,n})$. Therefore

$$\begin{aligned} u_{m_0,\infty} - u_{m_0,-\infty} &= \lim_{N \rightarrow \infty} (u_{m_0,N} - u_{m_0,-N}) = v_{m_0,n_0} - v_{m_0-1,n_0} \\ &+ \sum_{x \in M_+} h(x) e^{ix\xi_0} (1 - e^{-ix}) \frac{e^{ix\mu}}{e^{ix\mu} - 1} + \sum_{x \in M_-} h(x) e^{ix\xi_0} (1 - e^{-ix}) \frac{1}{e^{ix\mu} - 1}. \end{aligned}$$

We now consider two possibilities.

Case 1: $\xi_0 - 1 < 0$.

This case is possible only when $m_0 = -\mu(n_0 - 1) + 1$ so $\xi_0 = 1/2$. Using the fact that $x \in M_+$ whenever $x \in M_-$, we obtain

$$\begin{aligned} u_{m_0, \infty} - u_{m_0, -\infty} &= -\frac{1}{1 + \frac{\chi}{\mu^2}} + \sum_{x \in M_+} h(x) e^{ix\xi_0} \left\{ \frac{1 - e^{-ix}}{1 - e^{-ix\mu}} - 1 \right\} \\ &+ \sum_{x \in M_-} h(x) e^{ix\xi_0} \left\{ \frac{1 - e^{-ix}}{e^{ix\mu} - 1} - e^{-ix} \right\} = -\frac{1}{1 + \frac{\chi}{\mu^2}} - 2 \sum_{x \in M_+} h(x) \frac{\sin(\frac{1}{2}x(\mu - 1))}{\sin(\frac{1}{2}x\mu)} \end{aligned} \quad (67)$$

Compatibility condition can then be shown by considering the contour integral

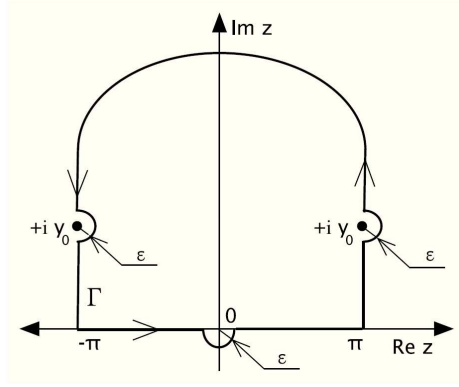


Figure 14: Contour Γ used in the proof of compatibility.

$$I = \int_{\Gamma} \frac{\sin \frac{1}{2}\mu z \sin \frac{1}{2}(\mu - 1)z}{\sin \frac{1}{2}z(\chi \sin^2 \frac{z}{2} + \sin^2 \frac{\mu z}{2})} dz$$

with contour Γ as shown in Fig. 14 and using the residue theorem. This yields

$$\frac{1 - 1/\mu}{1 + \chi/\mu^2} + -2 \sum_{x \in M_+} h(x) \frac{\sin(\frac{1}{2}x(\mu - 1))}{\sin(\frac{1}{2}x\mu)} = 0,$$

which together with (67) establishes (31).

Case 2: $\xi_0 - 1 > 0$.

In this case $m_0 = -\mu(n_0 - 1) + \nu$ with $\nu = 2, 3, \dots, \mu$, so $\xi_0 = \nu - 1/2$. Proceeding as in the previous case, we obtain

$$\begin{aligned} u_{m_0, \infty} - u_{m_0, -\infty} &= \sum_{x \in M_+} h(x) e^{ix\xi_0} (-1 + e^{-ix}) + \sum_{x \in M_+} h(x) e^{ix\xi_0} (1 - e^{-ix}) \frac{e^{ix\mu}}{e^{ix\mu} - 1} \\ &+ \sum_{x \in M_-} h(x) e^{ix\xi_0} \frac{1 - e^{-ix}}{e^{ix\mu} - 1} = 2 \sum_{x \in M_+} h(x) \cos(x(\nu - \mu/2 - 1)) \frac{\sin \frac{x}{2}}{\sin \frac{1}{2}x\mu} \end{aligned}$$

The compatibility can be proved similarly to the previous case by considering the contour integral

$$I = \int_{\Gamma} \frac{\sin \frac{1}{2}\mu z \cos(z(\nu - \mu/2 - 1))}{\chi \sin^2 \frac{z}{2} + \sin^2 \frac{\mu z}{2}} dz$$

with Γ as shown in Fig. 14.

B Asymptotic behavior of the off-diagonal entries of the tensor \mathbf{V} for sequential step propagation

In this appendix we reduce the double integral expression (55) for off-diagonal terms of tensor \mathbf{V} for sequential step propagation to a single integral and obtain the asymptotic behavior of these terms when $|j - k|$ is sufficiently large.

First observe that (55) can be rewritten as $V_{k,j} = I(|j - k|)$, where

$$I_k(\mu, \chi) = \frac{1}{\pi^2} \int_0^\pi \int_0^\pi \frac{\cos[\mu mx] \cos[my] \sin^2 \frac{y}{2}}{\chi \sin^2 \frac{x}{2} + \sin^2 \frac{y}{2}} dy dx \quad (68)$$

for integer $k \geq 0$. Consider the interior integral

$$\begin{aligned} \mathcal{L}_k(x, \chi) &= \frac{1}{\pi^2} \int_0^\pi \frac{\cos[ky] \sin^2 \frac{y}{2}}{\chi \sin^2 \frac{x}{2} + \sin^2 \frac{y}{2}} dy \\ &= \frac{1}{2} \int_{-\pi}^\pi \frac{\cos[ky] \sin^2 \frac{y}{2}}{\chi \sin^2 \frac{x}{2} + \sin^2 \frac{y}{2}} dy \end{aligned} \quad (69)$$

Following the procedure in [3] for a similar integral, we introduce a new variable $z = e^{iy}$ and define λ by (58). Note that $1 \leq \lambda \leq 1 + 2\chi$. We can now rewrite (69) as

$$\mathcal{L}_k(x, \chi) = \frac{1}{2\pi^2} (T_{k+1}(x, \chi) + T_{k-1}(x, \chi) - 2T_k(x, \chi)),$$

where

$$T_k = \oint_{|z|=1} \frac{z^m dz}{i(z^2 - 2\lambda z + 1)} \quad (70)$$

is the counterclockwise integral over the unit circle in the complex plane. Here we used the symmetry property of T : $T_k(x, \chi) = T_{-k}(x, \chi)$.

To evaluate (70) for $k \in \mathbb{Z}^+$ (off-diagonal entries of \mathbf{V}), observe that at $\lambda > 1$ the integrand has two real poles, $z = \lambda \pm \sqrt{\lambda^2 - 1}$. The pole $z = \lambda - \sqrt{\lambda^2 - 1}$ is inside the unit circle, and the other pole is outside. As $\lambda \rightarrow 1$, both poles approach $z = 1$ on the unit circle. Using residue theorem, we obtain, for $\lambda > 1$,

$$T_k(x, \chi) = -\pi \frac{(\lambda - \sqrt{\lambda^2 - 1})^k}{\sqrt{\lambda^2 - 1}},$$

and thus the interior integral (69) reduces to

$$\mathcal{L}_k(x, \chi) = -\frac{1}{\pi} \sqrt{\frac{\lambda - 1}{\lambda + 1}} (\lambda - \sqrt{\lambda^2 - 1})^k, \quad k \in \mathbb{Z}^+. \quad (71)$$

We can show that this formula works for $\lambda = 1$ as well. Using this expression and the fact that

$$I_k(\mu, \chi) = \int_0^\pi \cos(k\mu x) \mathcal{L}_k(x, \chi) dx, \quad (72)$$

we reduce the double integral (68) to the single integral (57).

We now construct an asymptotic expression for $I_k(\mu, \chi)$ at large k . To this end, observe that for $\lambda > 1$ ($x > 0$) we have $\lambda - \sqrt{\lambda^2 - 1} < 1$, so at large k $\mathcal{L}_k(x, \chi)$ decays fast away from $x = 0$. Hence the asymptotic behavior of the integral (57) is primarily determined by the behavior of $\mathcal{L}_k(x, \chi)$ at small x ($\lambda \approx 1$). Thus we approximate $\mathcal{L}_k(x, \chi)$ by the function $ax \exp(-bx)$, where the constants a and b are chosen so that the first two terms of the Taylor series of $ax \exp(-bx)$ and $\mathcal{L}_k(x, \chi)$ about $x = 0$ coincide. This yields

$$\mathcal{L}_k(x, \chi) \approx -\frac{\sqrt{\chi}}{2\pi} x e^{-\sqrt{\chi} k x}.$$

Substituting this approximation in (72), we can integrate exactly, obtaining

$$I_k(\mu, \chi) \approx \frac{\sqrt{\chi}(\mu^2 - \chi + (-1)^{\mu k} e^{-\sqrt{\chi} k \pi} (\chi - \mu^2 + \sqrt{\chi}(\chi + \mu^2)\pi k))}{2(\chi + \mu^2)^2 k^2 \pi}. \quad (73)$$

Clearly, the approximation improves at larger k . At large k for $\chi \neq \mu^2$ the dominant term is

$$\frac{\sqrt{\chi}(\mu^2 - \chi)}{2(\chi + \mu^2)^2 k^2 \pi},$$

so $I_k(\mu, \chi) = O(1/k^2)$. This implies that at $\mu^2 > \chi$ and sufficiently large m the off-diagonal terms are positive. Meanwhile $\mu^2 < \chi$ means negative off-diagonal terms at least for large enough m . In fact, numerical evaluation of the exact integral (57) at various parameters satisfying $\mu^2 < \chi$ shows that all off-diagonal terms are negative in this case.

C Proofs of propositions in Section 8

Proof of Proposition 1:

(a) We have

$$\left| \sum_{j=1}^k I_j(\mu, \chi) \right| \leq \sum_{j=1}^k |I_j(\mu, \chi)| \leq \frac{1}{\pi} \int_0^\pi \sqrt{\frac{\lambda-1}{\lambda+1}} \sum_{j=1}^k \frac{1}{(\lambda + \sqrt{\lambda^2 - 1})^j} dx.$$

Therefore

$$\left| \sum_{j=1}^k I_j(\mu, \chi) \right| < \frac{1}{\pi} \int_0^\pi \sqrt{\frac{\lambda-1}{\lambda+1}} \sum_{j=1}^\infty \frac{1}{(\lambda + \sqrt{\lambda^2 - 1})^j} dx = J_*(\chi).$$

It can be shown that $J_*(\chi) = \frac{1}{2\pi} \int_0^\pi (1 - \sqrt{\frac{\lambda-1}{\lambda+1}}) dx = \frac{1}{2} V_{1,1}$, and (a) follows. This clearly implies that $|I_k(\mu, \chi)| < \frac{1}{2} V_{1,1}$ for all $k \in \mathbb{Z}^+$.

(b) Note that (a) also implies that $\lim_{k \rightarrow \infty} I_k(\mu, \chi) \rightarrow 0$. Monotonicity of $I_k(\mu, \chi)$ at large k and $\chi \neq \mu^2$ follows immediately from the asymptotic expression (73) obtained in Appendix C at large $k \in \mathbb{Z}^+$.

(c) To prove this part, observe that I_k can be written as (72), with the amplitude $\mathcal{L}_k(x, \chi)$ of the integrand given by (71). From (58) it follows that $\mathcal{L}_k(x, \chi) \leq 0$. The smoothness of this function at $\chi > 0$ and $x \in [0, \pi]$ ensures that I_k can be differentiated under the integral at $\chi > 0$. Since I_k depends on χ only through $\mathcal{L}_k(x, \chi)$, this dependence is determined by the properties of $\mathcal{L}_k(x, \chi)$. Simple analysis reveals that as a function of x for given χ , \mathcal{L}_k has a single minimum point. If

$$\chi \leq \frac{\sqrt{1+k^2} - k}{2k},$$

the minimum is reached at $x = \pi$. Otherwise, the minimum depends only on k and is attained at

$$x_*(k, \chi) = 2 \arcsin \sqrt{\frac{\sqrt{1+k^2} - k}{2\chi k}} < \pi,$$

and \mathcal{L}_k is a convex function of x in the interval $(0, x_*)$.

We claim that $I_k < 0$ for large χ . By definition

$$I_k(\mu, \chi) = -I_k^{(1)}(\mu, \chi) + I_k^{(2)}(\mu, \chi),$$

with $I_k^{(1)}(\mu, \chi) = -\int_0^{\frac{\pi}{2k\mu}} \mathcal{L}_k(x, \chi) \cos(k\mu x) dx$ and $I_k^{(2)}(\mu, \chi) = \int_{\frac{\pi}{2k\mu}}^{\pi} \mathcal{L}_k(x, \chi) \cos(k\mu x) dx$.

Let $\hat{\lambda} = \lambda(\frac{\pi}{2k\mu}, \chi)$. For large enough $\chi > 0$ such that $x_* < \frac{\pi}{2k\mu}$, we have

$$I_k^{(2)}(\mu, \chi) < \left(1 - \frac{1}{2k\mu}\right) \sqrt{\frac{\hat{\lambda}-1}{\hat{\lambda}+1}} (\hat{\lambda} - \sqrt{\hat{\lambda}^2 - 1})^k = \frac{C_k^{(2)}(\mu)}{\chi^k} + o\left(\frac{1}{\chi^k}\right),$$

at large χ , where

$$C_k^{(2)}(\mu) = \left(1 - \frac{1}{2k\mu}\right) \frac{1}{4^k \sin^{2k} \frac{\pi}{2k\mu}} > 0$$

for $\mu, k \in \mathbb{Z}^+$. Since $x_* < \frac{\pi}{2k\mu}$, the integrand in $I_k^{(1)}$ is nonnegative. Using this along with convexity of \mathcal{L}_k in the interval $(0, x_*)$, we obtain

$$I_k^{(1)}(\mu, \chi) > -\cos(k\mu x_*) \int_0^{x_*} \mathcal{L}_k(x, \chi) dx > -\frac{1}{2} \mathcal{L}_k^* x_* \cos(\mu k x_*),$$

where $\mathcal{L}_k^* \equiv \mathcal{L}_k(x_*(\chi, k), \chi)$ is independent of χ . Hence at large χ

$$I_k^{(1)}(\mu, \chi) > \frac{C_k^{(1)}}{\sqrt{\chi}} + o\left(\frac{1}{\sqrt{\chi}}\right),$$

where

$$C_k^{(1)} = \frac{1}{\pi} \left(\frac{\sqrt{1+k^2}}{k} - 1 \right) \left(\frac{\sqrt{1+k^2}-1}{k} \right)^k \sqrt{1 - 2k(\sqrt{1+k^2}-k)} > 0$$

The claim that $I_k < 0$ for large χ follows immediately. At small $\chi > 0$ we have

$$\frac{\partial \mathcal{L}_k}{\partial \chi} \approx -\frac{1}{2\pi\sqrt{\chi}} \sin \frac{x}{2},$$

so

$$\frac{\partial I_k}{\partial \chi} \approx -\frac{1}{2\pi\sqrt{\chi}} \int_0^{\pi} \sin \frac{x}{2} \cos(k\mu x) dx = -\frac{1}{\pi\sqrt{\chi}(1-4\mu^2 k^2)} > 0,$$

since $\mu, k \in \mathbb{Z}^+$. This and $I_k(\mu, 0) = 0$ imply that $I_k(\mu, \chi) > 0$ for small χ . By continuity of I_k and intermediate value theorem there exists $\chi_k(\mu) > 0$ such that $I_k(\mu, \chi_k(\mu)) = 0$

and $I_k(\mu, \chi_k(\mu)) > 0$ for $0 < \chi < \chi_k(\mu)$. This concludes the proof.

Proof of Proposition 2:

(a) First, note that for $b \leq 1$ we have

$$\mathcal{K}_k(b, \mu, x) \rightarrow \frac{b(b - \cos(\mu x))}{2b \cos(\mu x) - b^2 - 1}$$

as $k \rightarrow \infty$. Using the fact that $b = \lambda - \sqrt{\lambda^2 - 1} \leq 1$, we can show that

$$J_\infty(\mu, \chi) \equiv \lim_{k \rightarrow \infty} J_k(\mu, \chi) = \frac{\arctan \sqrt{\chi}}{\pi} - \frac{\chi}{2\pi} \int_0^\pi \frac{\sin^2 \frac{x}{2} dx}{\sin^2 \frac{\mu x}{2} + \chi \sin^2 \frac{x}{2}}. \quad (74)$$

From (63) it follows that $\Delta E_\infty(\mu, \chi) > \Delta E_1(\mu, \chi)$ if and only if $J_\infty(\mu, \chi) > 0$ and $\Delta E_\infty(\mu, \chi) = \Delta E_1(\mu, \chi)$ if and only if $J_\infty(\mu, \chi) = 0$. Applying the residue theorem to evaluate the integral in (74), we obtain the transcendental equation (64) that determines $\chi_*(\mu)$.

(b) If $\chi < \chi_1(\mu)$, the Corollary to the conjecture following Proposition 1 and the definition of J_k imply that $J_{k+1} - J_k = V_{k+1,1} = I_k > 0$ for all $m \in \mathbb{Z}^+$. Hence $J_k(\mu, \chi)$ monotonically increase with k to the limiting value $J_\infty(\mu, \chi)$. From (63) it follows that ΔE_k must monotonically decrease in this range of χ . Similarly, the same Corollary implies $J_{k+1} < J_k$ for all $m \in \mathbb{Z}^+$ if $\chi > \mu^2$, so that the energy barriers monotonically increase. Finally, if $\chi_1 \leq \chi \leq \mu^2$ and k_* is such that $\chi_{k_*-1}(\mu) \leq \chi < \chi_{k_*}(\mu)$, the Corollary implies that $J_k \leq J_{k-1}$ for $k \leq k_*$ and $J_k > J_{k-1}$ for $k > k_*$, which results in the maximum energy barrier at $k = k_*$. This completes the proof.

Proof of Proposition 3:

We start with two general observations that hold for any $\chi > 0$, $\mu \in \mathbb{Z}$ and $n \in \mathbb{Z}_+$. First, Proposition 1(a) implies that

$$\sum_{i=1}^{n+1} \sum_{j=1}^{n+1} V_{i,j} - \sum_{i=1}^n \sum_{j=1}^n V_{i,j} = V_{1,1} + 2 \sum_{k=1}^n I_k > 0,$$

and therefore

$$\sum_{i=1}^{n+1} \sum_{j=1}^{n+1} V_{i,j} > \sum_{i=1}^n \sum_{j=1}^n V_{i,j}. \quad (75)$$

Second, note that

$$\left| \max_{1 \leq i \leq n} \sum_{j=1}^n V_{i,j} \right| \leq V_{1,1} + 2 \sum_{k=1}^{n-1} |I_k| < 2V_{1,1}, \quad (76)$$

where the second inequality follows from Proposition 1(a).

Now consider

$$R_n = \frac{\Delta E}{\Delta E_1} = \frac{V_{1,1} \sum_{i,j=1}^n V_{i,j}}{\left(\max_{1 \leq i \leq n} \sum_{j=1}^n V_{i,j} \right)^2}.$$

We need to show that $R_n > 1$ for all integer $n \geq 2$. We consider the following three cases.

Case I: $\chi \geq \mu^2$

Recall that in this case $I_k < 0$ for $n \in \mathbb{Z}_+$, by the first part of the corollary to the conjecture following Proposition 1. Hence $\max \sum_{j=1}^n V_{i,j} \leq V_{1,1}$, and by (75), we have $\sum_{i=1}^n \sum_{j=1}^n V_{i,j} > nV_{1,1}$ for $n \geq 2$. Thus $R_n > 1$.

Case II: $\chi \leq \chi_1(\mu)$

In this case $I_1 \geq 0$ and $I_k > 0$ for $k \geq 2$. Thus

$$\sum_{i=1}^n \sum_{j=1}^n V_{i,j} = nV_{1,1} + 2 \sum_{k=1}^{n-1} (n-k)I_k > nV_{1,1}.$$

Using (76), we obtain

$$R_n > \frac{n}{4} > 1$$

if $n > 4$. The cases $n = 2, 3$ and 4 will be considered separately. For $n = 2$,

$$R_2 = \frac{2V_{1,1}(V_{1,1} + I_1)}{(V_{1,1} + I_1)^2} = \frac{2V_{1,1}}{(V_{1,1} + I_1)} > 1$$

because $I_1 < V_{1,1}$. For $n = 3$, we write

$$\max_{1 \leq i \leq 3} \sum_{j=1}^3 V_{i,j} = V_{1,1} + S,$$

where S is given by either $S = 2I_1 \geq 0$ or $S = I_1 + I_2 > 0$. If $S = 2I_1$, $\sum_{i=1}^3 \sum_{j=1}^3 V_{i,j} = 3V_{1,1} + 4I_1 + 2I_2 > 2V_{1,1} + 4I_1$, so that

$$R_3 > \frac{2V_{1,1}(V_{1,1} + 2I_1)}{(V_{1,1} + 2I_1)^2} = \frac{(V_{1,1} + 2I_1)^2 + V_{1,1}^2 - 4I_1^2}{(V_{1,1} + 2I_1)^2} > 1$$

since $I_1 < V_{1,1}/2$ and thus $V_{1,1}^2 > 4I_1^2$. If $S = I_1 + I_2$, we write $\sum_{i=1}^3 \sum_{j=1}^3 V_{i,j} > 2(V_{1,1} + S)$ and hence

$$R_3 > \frac{2V_{1,1}(V_{1,1} + S)}{(V_{1,1} + S)^2} = \frac{(V_{1,1} + S)^2 + V_{1,1}^2 - S^2}{(V_{1,1} + S)^2} > 1$$

since $S^2 < V_{1,1}^2$. The proof of $R_4 > 1$ is similar.

Case III: $\chi_1(\mu) < \chi < \mu^2$

In this case the second part of the corollary states that there exists an integer $k_* \geq 2$ such that $I_k < 0$ for $k < k_*$, $I_{k_*} \leq 0$ and $I_k > 0$ for $k > k_*$. Consequently, there exists $n_* > k_*$ ($n_* \geq 3$) such that $\sum_{k=1}^n (n-k)I_k \geq 0$ for $n \geq n_*$ and $\sum_{k=1}^n (n-k)I_k < 0$ for $n < n_*$.

For $n < k_*$ the situation is the same as in Case I (all I_k are negative), and we can prove that $R_n > 1$. For $n \geq n_* + 1$ we can use (75) repeatedly along with the definition of n_* to obtain

$$\sum_{i=1}^n \sum_{j=1}^n V_{i,j} > \sum_{i=1}^{n_*+1} \sum_{j=1}^{n_*+1} V_{i,j} = (n_* + 1)V_{1,1} + 2 \sum_{k=1}^{n_*} (n-k)I_k \geq (n_* + 1)V_{1,1}.$$

Using this and (76), we have

$$R_n > \frac{n_* + 1}{4} \geq 1,$$

since $n_* \geq 3$. Finally, consider n such that $k_* \leq n \leq n_*$. In this case we have $\sum_{k=1}^{n-1} (n-k)I_k < 0$. Since the sum of entries in all rows of \mathbf{V} is greater than the maximum sum of entries in a row, and each row contains $V_{1,1}$, we have

$$\max_{1 \leq i \leq n} \sum_{j=1}^n V_{i,j} < 2 \sum_{k=1}^{n-1} (n-k)I_k + V_{1,1}.$$

Since $n \geq 2$, this yields

$$R_n > \frac{V_{1,1}(nV_{1,1} + 2 \sum_{k=1}^{n-1} (n-k)I_k)}{(V_{1,1} + 2 \sum_{k=1}^{n-1} (n-k)I_k)^2} > \frac{V_{1,1}}{V_{1,1} + 2 \sum_{k=1}^{n-1} (n-k)I_k} > 1,$$

due to the negative sum in the denominator. Thus $R_n > 1$ for all $n \geq 2$ in Case III.

References

- [1] D.W. Bray and J.M. Howe. High-resolution transmission electron microscopy investigation of the face-centered cubic/hexagonal close-packed martensite transformation in Co-31.8 Wt Pct Ni alloy: Part I. Plate interfaces and growth ledges. *Metall. Mat. Trans. A*, 27A:3362–3370, 1996.
- [2] J. W. Cahn, J. Mallet-Paret, and E. S. Van Vleck. Traveling wave solutions for systems of odes on a two-dimensional spatial lattice. *SIAM Journal on Applied Mathematics*, 59(2):455–493, 1998.

- [3] V. Celli and N. Flytzanis. Motion of a screw dislocation in a crystal. *Journal of Applied Physics*, 41(11):4443–4447, 1970.
- [4] R. J. Duffin. Discrete potential theory. *Duke Mathematical Journal*, 20:233–251, 1953.
- [5] B. Fedelich and G. Zanzotto. Hysteresis in discrete systems of possibly interacting elements with a two well energy. *Journal of Nonlinear Science*, 2:319–342, 1992.
- [6] J. P. Hirth and J. Lothe. *Theory of dislocations*. John Wiley and Sons, 1982.
- [7] J.P. Hirth. Ledges and dislocations in phase transformations. *Metall. Mat. Trans. A*, 25A:1885–1894, 1994.
- [8] R. Hobart. A solution to the Frenkel-Kontorova dislocation model. *Journal of Applied Physics*, 33(1):60–62, 1962.
- [9] R. Hobart. Peierls-barrier minima. *Journal of Applied Physics*, 36(6):1948–1952, 1965.
- [10] R. Hobart. Peierls stress dependence on dislocation width. *Journal of Applied Physics*, 36(6):1944–1948, 1965.
- [11] R. Hobart. Peierls-barrier analysis. *Journal of Applied Physics*, 37(9):3572–3576, 1966.
- [12] A. A. Maradudin. Screw dislocations and discrete elastic theory. *Journal of Physics and Chemistry of Solids*, 9(1):1–20, 1958.
- [13] L. Truskinovsky and A. Vainchtein. Peierls-nabarro landscape for martensitic phase transitions. *Physical Review B*, 67:172103, 2003.
- [14] Y. Zhen and A. Vainchtein. Dynamics of steps along a martensitic phase boundary I: Semi-analytical solution. 2007. In preparation.
- [15] Y. Zhen and A. Vainchtein. Dynamics of steps along a martensitic phase boundary II: Numerical simulations. 2007. In preparation.